

# Diversified natural products in *Rhododendron formosanum* reveal allelochemical and pharmaceutical properties

Chang-Hung Chou<sup>1</sup>, Tzong-Der Way<sup>2</sup>, Shang-Jie Tsai<sup>1</sup>, Yun-Lian Jhan<sup>1</sup> and Chao-Min Wang<sup>1</sup>

<sup>1</sup>Research Center for Biodiversity, China Medical University, Taichung, Taiwan

<sup>2</sup>Department of Biological Science and Technology, College of Biopharmaceutical and Food Sciences, China Medical University, Taichung, Taiwan

**Chair Professor and Director**  
**Research Center for Biodiversity, China Medical University,**  
**Taichung, Taiwan**

**5th International Conference on Biodiversity**  
**March 10-12, 2016, Madrid, Spain**



China Medical University

# **Plant Natural Products Play Important Roles in Plant Ecosystem**

- **Dominance of vegetation**
- **Climax species**
- **Mechanism of plant succession**
- **Plant productivity**
- **Regulation of biodiversity**



*Allelopathy Journal* 25 (1): 73-92 (2010)  
Tables: 4, Figs : 11

*International Allelopathy Foundation* 2010

## **Allelopathic potential of *Rhododendron formosanum* Hemsl in Taiwan**

S.C. CHOU, C.H. HUANG, T.W. HSU<sup>1</sup>, C.C. WU<sup>2</sup> and C.H. CHOU\*

Research Center for Biodiversity and Graduate Institute of Ecology and  
Evolutionary Biology, China Medical University, Taichung 40402, Taiwan  
E. Mail: [choumasa@mail.cmu.edu.tw](mailto:choumasa@mail.cmu.edu.tw)



China Medical University

## *Rhododendron formosanum*

- Endemic specie in Taiwan
- Small trees to 10 m tall
- 600~2400 m asl.
- The soil is acidic (pH 4.0)
- Nitrogen availability is limited





China Medical University

Dasyueshan site ( $24^{\circ}14'6.49''\text{N}$ ,  $120^{\circ}57'7.29''\text{E}$   
at 1911 m asl.; annual rainfall: 2000–3000 mm)



Figure 1. An almost lacking understory plant on the floor of *R. formosanum* (A) as compared to many understory plants on the floor of adjacent woody plant, *C. cuspidata* var. *carlesii* (B), at the Sun Link Sea study site in April, 2008.



Table 1. Comparison of floristic composition and relative coverage of each understory species found on the floors of *C. cuspidata* var. *carlesii* and *R. formosanum* in the Sun Link Sea site

Species	Coverage (%) / Species	
	<i>C. cuspidata</i> var. <i>carlesii</i>	<i>R. formosanum</i>
<i>Acrophorus stipellatus</i> T. Moore	13.1	-
<i>Arachniodes rhomboides</i> (Wall. ex Mett.) Ching	18.1	-
<i>Ardisia crenata</i> Sims	1.1	-
<i>Callicarpa formosana</i> Folfe	6.8	-
<i>Diplazium kawakamii</i> Hayata	1.5	-
<i>Elatostema lineolatum</i> Wight var. <i>majus</i> Wedd.	1.2	-
<i>Eurya crenatifolia</i> (Yamam.) Kobuski	1.6	-
<i>Hemiboea bicornuta</i> (Hayata) Ohwi	2.0	-
<i>Hydrangea angustipetala</i> Hayata	0.5	-
<i>Monachosorum henryi</i> Chist	31.8	-
<i>Nanocnide japonica</i> Blume	0.2	-
<i>Pileostegia viburnoides</i> Hook. f. & Thomson	4.2	-
<i>Plagiogyria japonica</i> Nakai	4.7	-
<i>Rubus formosensis</i> Kuntze	0.3	-
<i>Smilax sieboldii</i> Miq.	0.5	-
<i>Stauntonia obovatifoliola</i> Hayata	0.1	-
<i>Strobilanthes formosanus</i> S. Moore	13.2	-
<i>Symplocos caudata</i> Wall. ex G. Don	4.5	-
<i>Vandenboschia auriculata</i> (Blume) Copel.	0.5	-
<i>Barthea barthei</i> (Hance) Krass	-	0.4
<i>Cinnamomum subavenium</i> Miq.	-	0.0
<i>Cleyera japonica</i> Thunb. <i>Damnacanthus angustifolius</i> Hayata	-	1.0
<i>Dendropanax dentiger</i> (Harms ex Diels) Merr. <i>Machilus thunbergii</i> Siebold & Zucc.	-	3.5
<i>Myrsine stolonifera</i> (Koidz.) Walker	-	0.1
<i>Neolitsea acuminatissima</i> (Hayata) Kaneh. & Sasaki	-	0.3
<i>Plagiogyria dunnii</i> Copel.	-	0.6
<i>Rhododendron formoscanum</i> Hemsl.	-	0.5
<i>Smilax lanceifolia</i> Roxb.	-	3.6
<i>Shortia rotundifolia</i> (Maxim.) Makino	-	1.6
Average total coverage (%)	105.7	1.7
Relative coverage of understory (%)	100.0	0.2
Number of species	19	12
- : Absent		





Figure 2. The leaching apparatus system: Upper part is a plastic tray, 55×40×15 cm with numerous needle-sized holes (2 cm between holes) was filled with tap water, which dripped through the holes to make an artificial raindrop, middle part is the same as upper tray, was filled with chopped plant material/organic matter to receive the artificial raindrop from upper tray, lower part is a plastic tray, like that of upper and middle tray, without holes to receive plant leachate from middle tray. The pump re-circulated the water from lower tray to upper tray

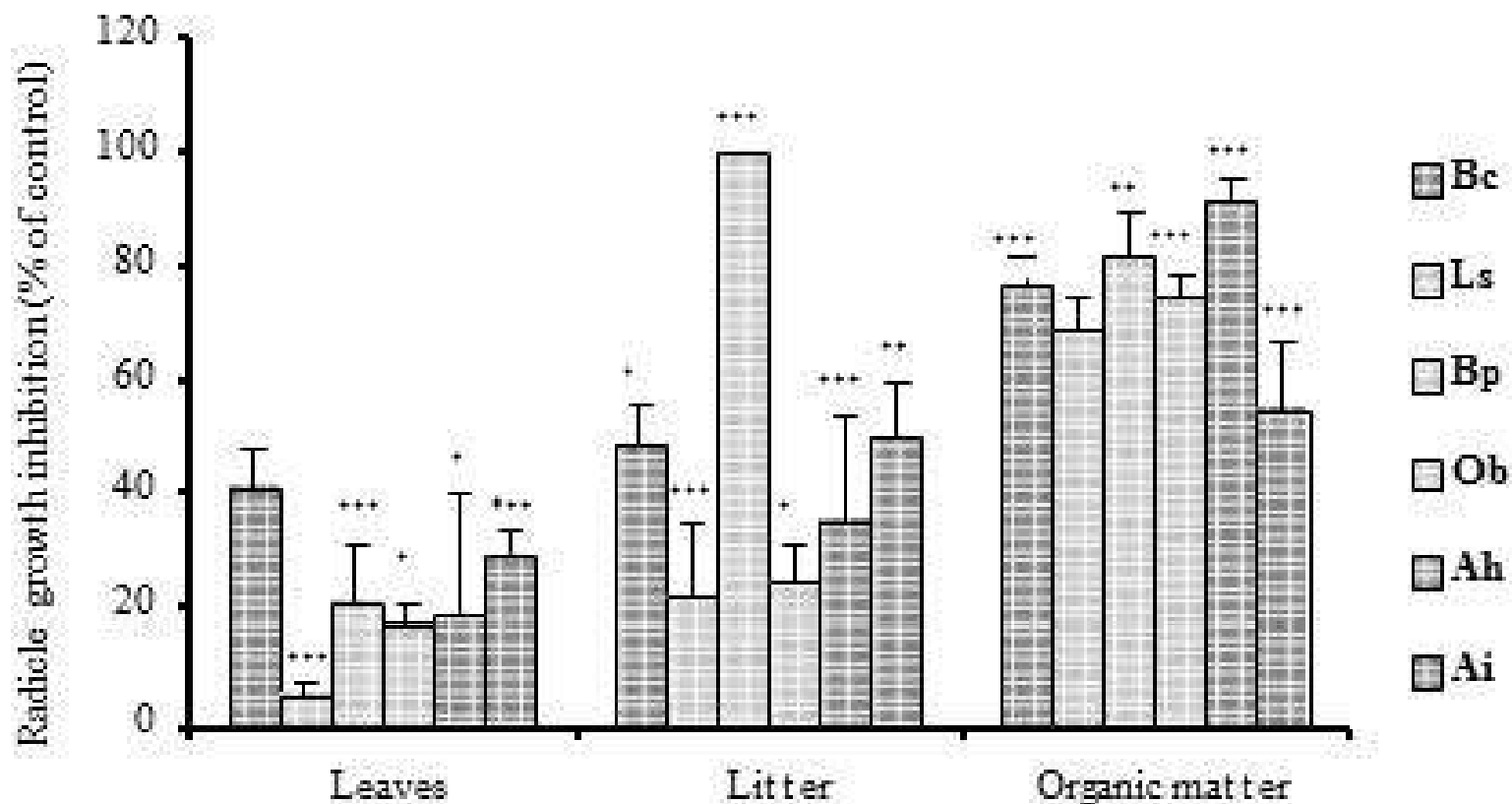


Figure 4. Effects of aqueous leachates of *Rhododendron* leaves, litter, and organic matter on the radicle growth of six bioassay species. Levels of statistical significance are expressed by asterisk: \* <math><0.05</math>, \*\* <math><0.01</math>, \*\*\* <math><0.001</math>. The abbreviations of species names are: *Ageratum houstonianum* (Ah), *Amaranthus inamoenus* (Ai), *Brassica chinensis* (Bc), *Bidens pilosa* (Bp), *Lactuca sativa* (Ls) and *Ocimum basilicum* (Ob)



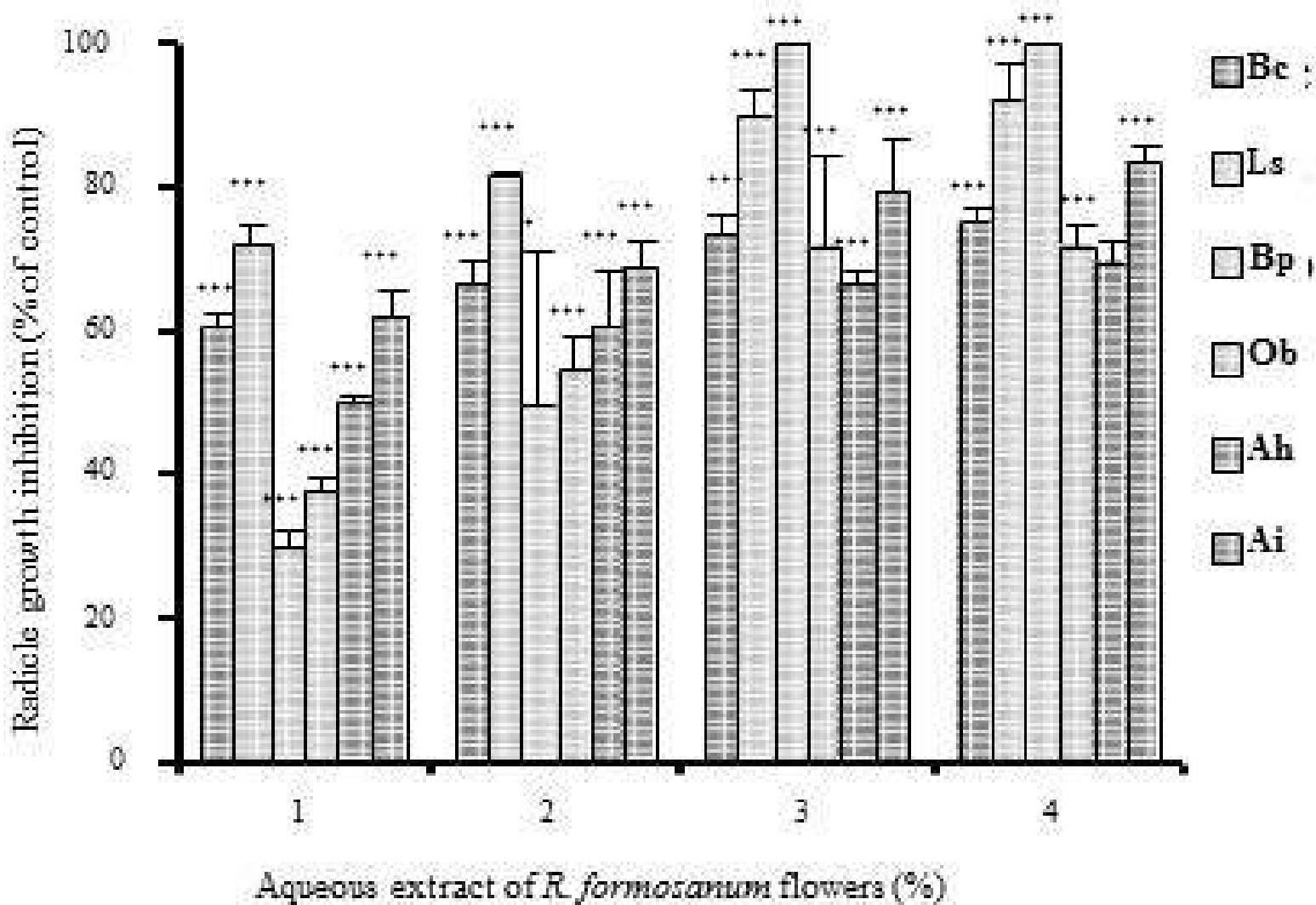


Figure 5. Effects of aqueous extracts concentration of *R. formosanum* flowers on radicle growth of six bioassay species. The abbreviations of legends see Figure 4.



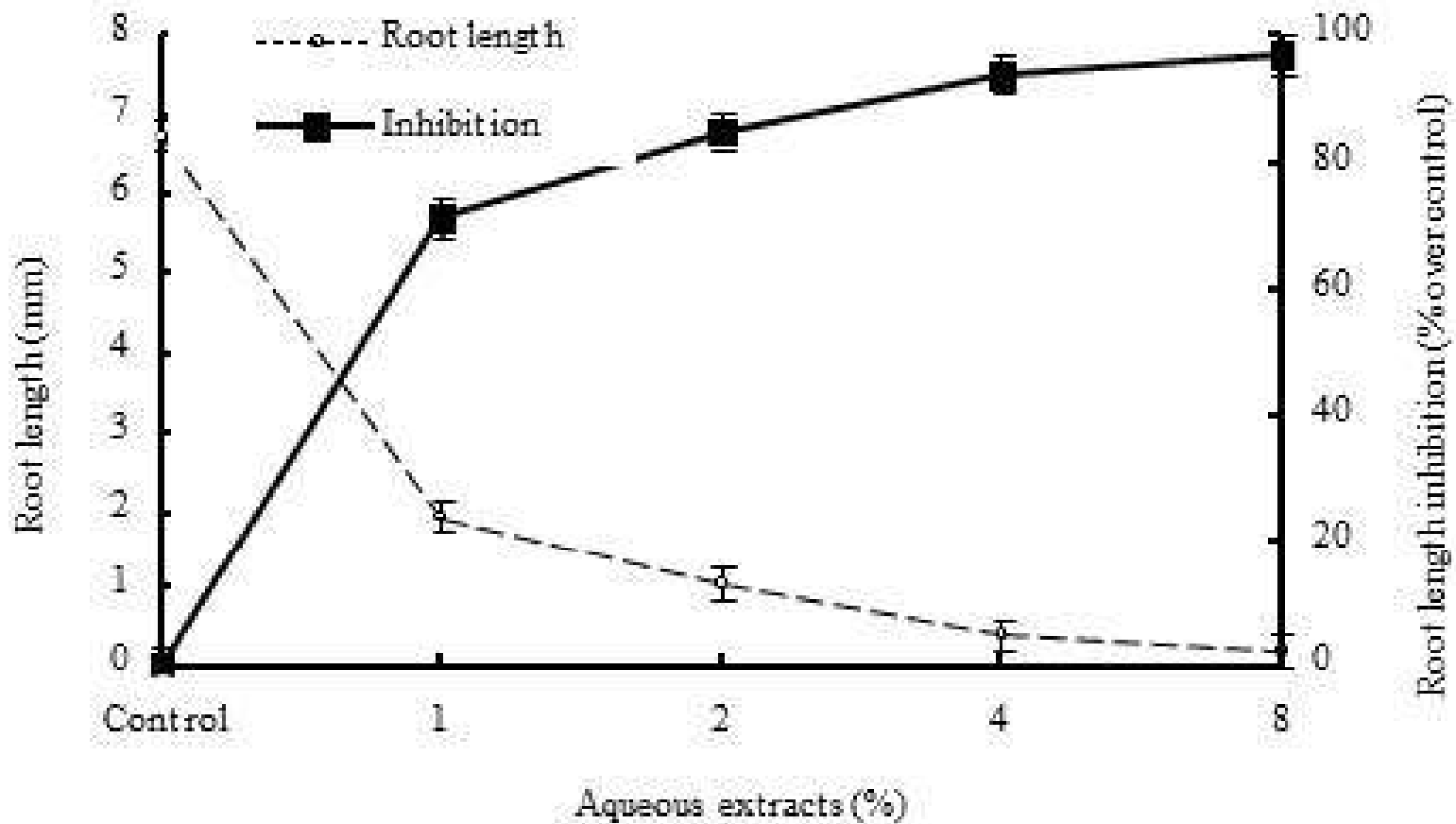


Figure 9. The inhibitory effect of aqueous extract, 0, 1, 2, 4 and 8 % of *R. formosanum* leaves on root length of root initiation of *B. mutica*. The inhibition was significantly different from distilled water control at 5 % level using Student's *t*-test.



Table 4. Phytotoxins isolated from the leaves of *Rhododendron formosanum* in Taiwan\*

Compound	R <sub>f</sub> values in paper chromatography (2 % HOAc)			HPLC	
	Authentic standard	Isolated from <i>Rhododendron</i> leaves	Relatively quantitative comparison**	Compound present	Peak number
<i>p</i> -Hydroxybenzoic acid	0.63	0.66	+	+	(5)***
Chlorogenic acid	0.67			+	(4)
<i>trans p</i> -Coumaric acid	0.43			+	(10)
<i>cis</i> Ferulic acid	0.64	0.68	+++		
Methyl ferulate	0.61	0.61	+	+	(13)
Syringic acid		0.56	++		
Vanillic acid	0.56	0.60	++	+	(6)
Coumarin	0.73			+	(12)
Protocatechuic acid	0.63	0.56	+	+	(2)
(-)-Catechin	0.46	0.47	++	+	(3)

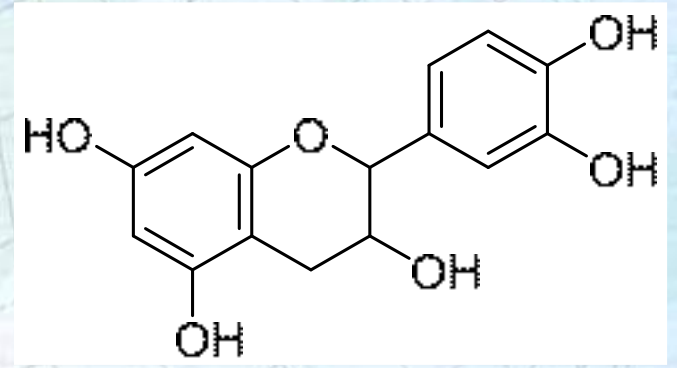
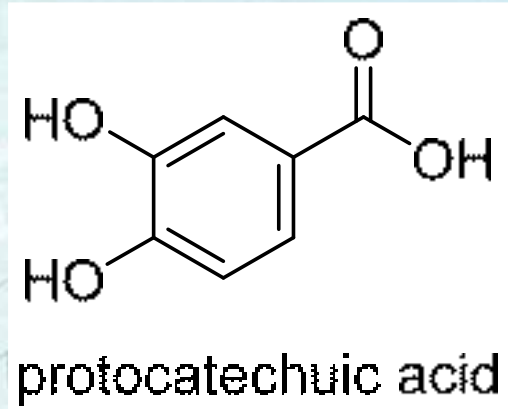
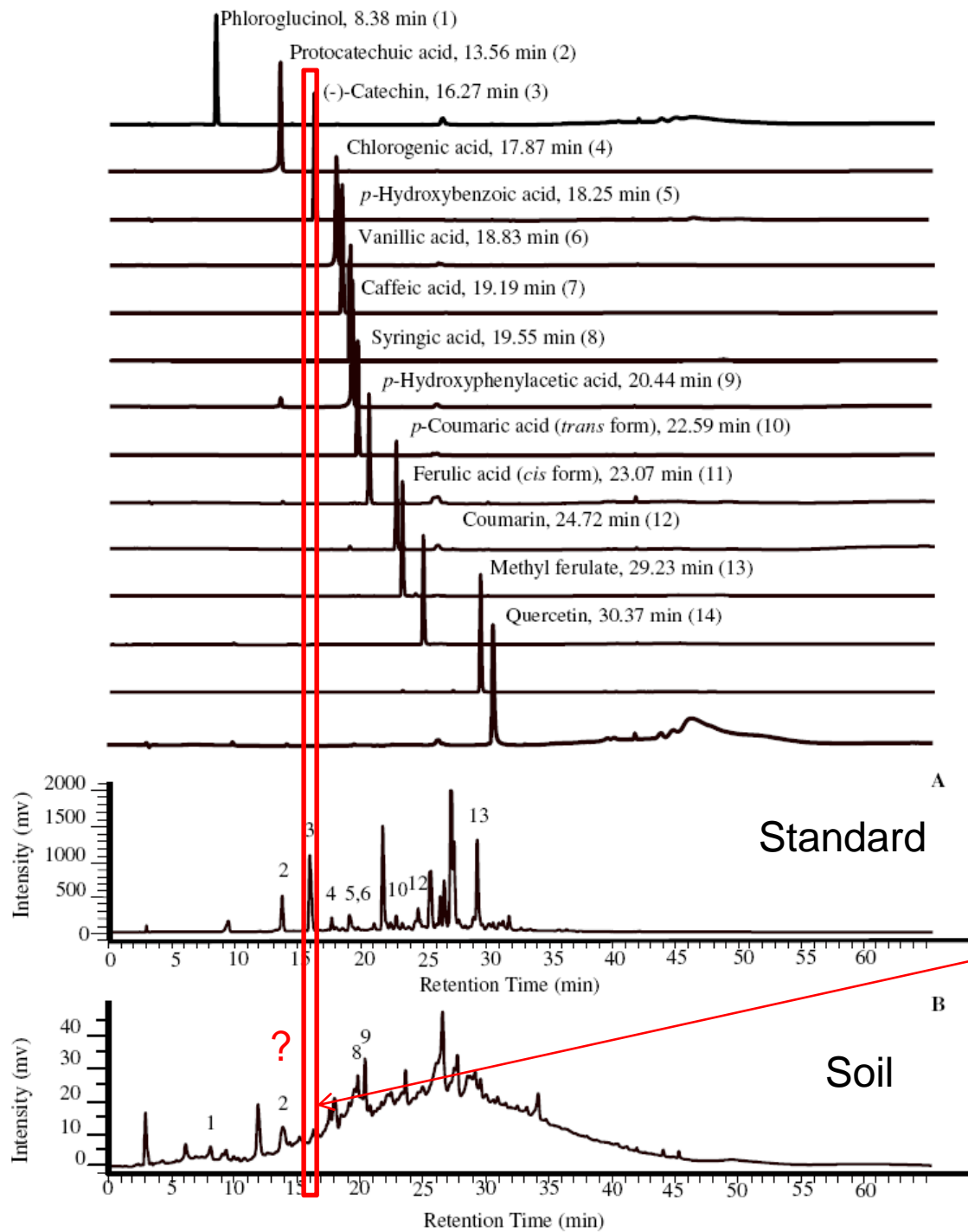
\* The identification is primarily based on PC and HPLC.

\*\* The amount of compound is based on the intensity of spot on the PC, showing +++ > ++ > +.

\*\*\* Data in parenthesis indicate the number of compound as compared to the authentic peak shown in Figure 11, the peak intensity that is larger than 200 mv in HPLC chromatogram is consider as +.

Chou et al., 2010





**Catechin degradation**

# The Impact of Microbial Biotransformation of Catechin in Enhancing the Allelopathic Effects of *Rhododendron formosanum*

Chao-Min Wang<sup>1</sup>, Tsai-Chi Li<sup>1</sup>, Yun-Lian Jhan<sup>2</sup>, Jen-Hsien Weng<sup>2</sup>, Chang-Hung Chou<sup>1,2,3\*</sup>

**1** Research Center for Biodiversity, China Medical University, Taichung, Taiwan, **2** Graduate Institute of Ecology and Evolutionary Biology, China Medical University, Taichung, Taiwan, **3** Department of Life Sciences, National Cheng Kung University, Tainan, Taiwan

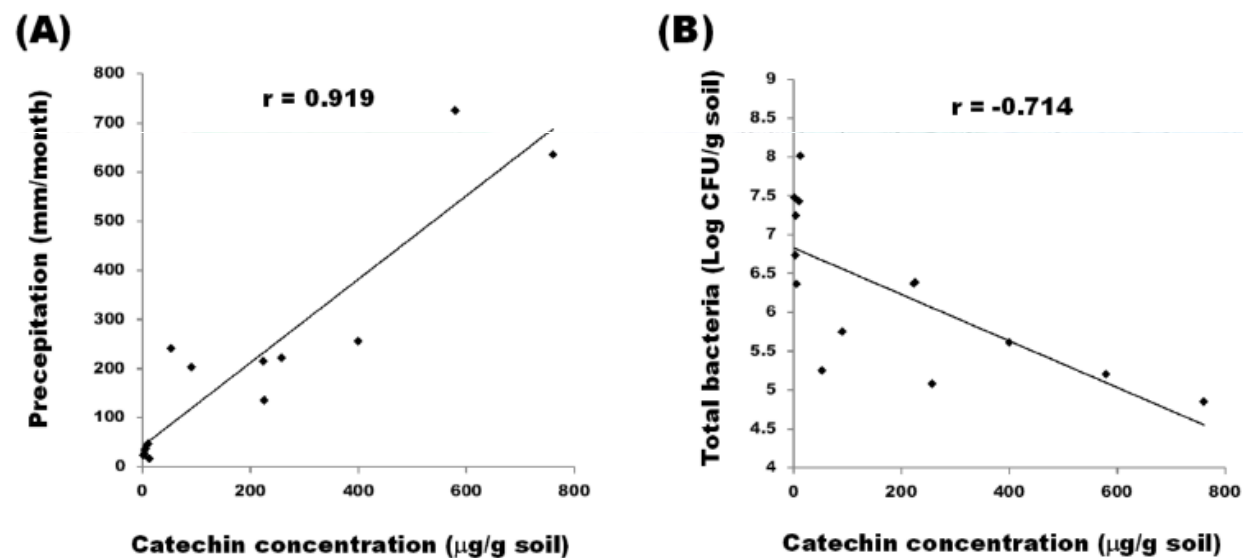


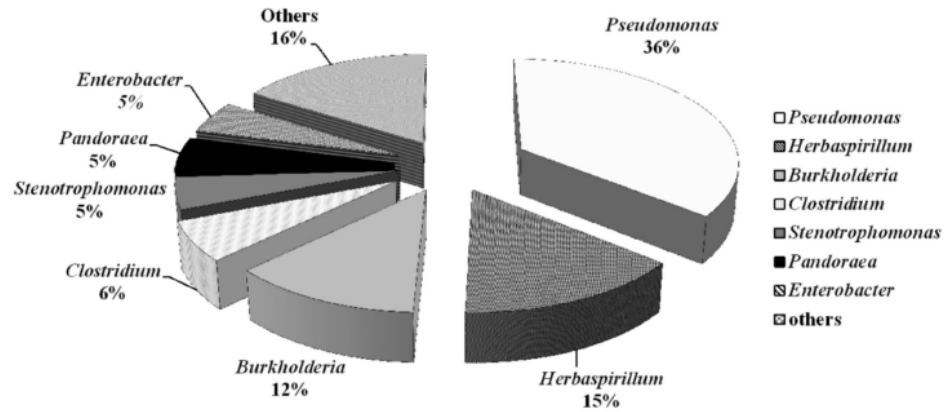
**Figure 1. Pairwise correlations between (-)-catechin concentration, monthly precipitation, and bacterial populations.** (A) Correlation between the concentration of (-)-catechin in soil of *R. formosanum* and monthly precipitation ( $r = 0.919$ ,  $P < 0.0001$ ,  $n = 14$ ). (B) Correlation between the concentration of (-)-catechin and bacterial populations in soil of *R. formosanum* ( $r = -0.714$ ,  $P = 0.0041$ ,  $n = 14$ ).

doi: 10.1371/journal.pone.0085162.g001



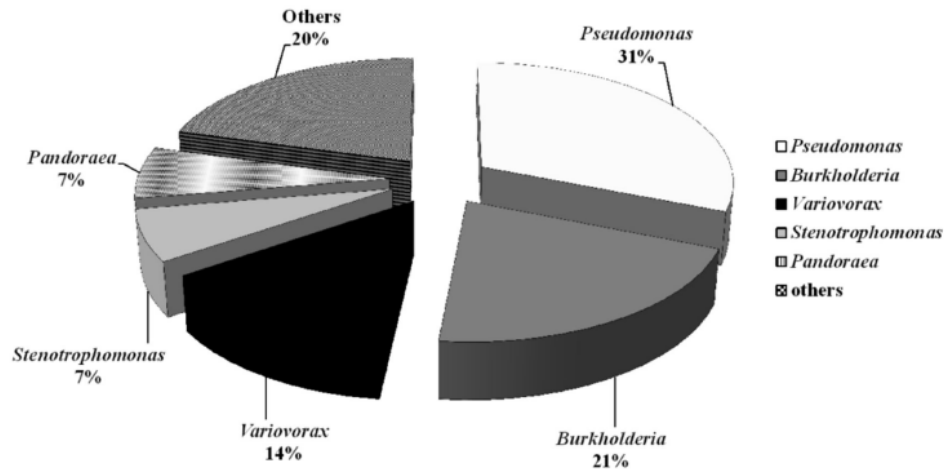
(A)

### Bacterial flora in soil of *R. formosanum*



(B)

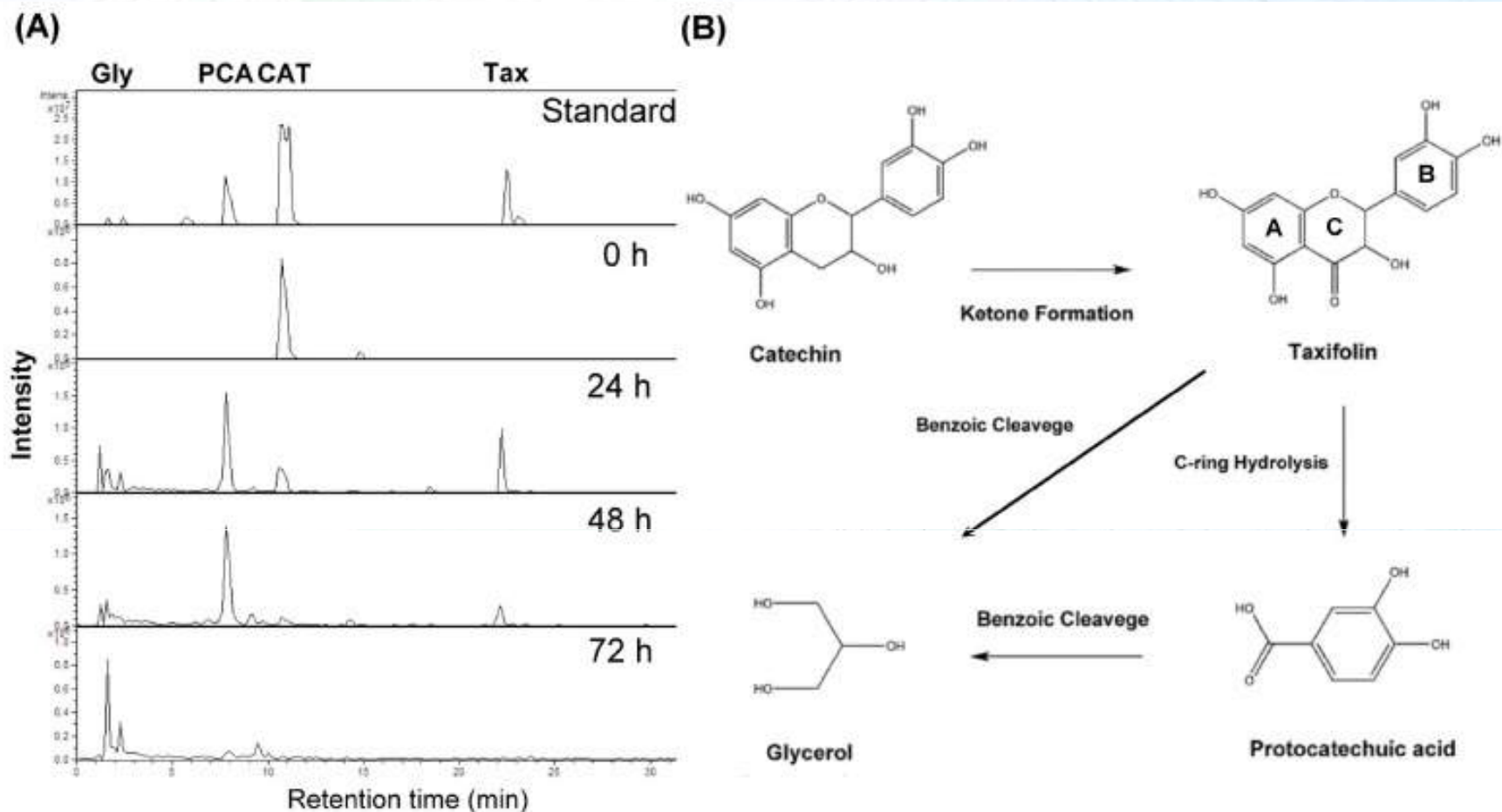
### Catechin-Utilizing Bacteria



**Figure 2. Bacterial flora (A) and catechin utilizing bacteria (B) in the rhizosphere of a *Rhododendron formosanum* plantation.** (-)Catechin was the only carbon source added to the medium that was used for microbial isolation. After 3 months of incubation, *Pseudomonas* spp., *Burkholderia* spp., *Variovorax* spp. *Stenotrophomonas* spp., and *Pandoraea* spp. were isolated and identified as dominant catechin-utilizing bacteria.

doi: 10.1371/journal.pone.0085162.g002

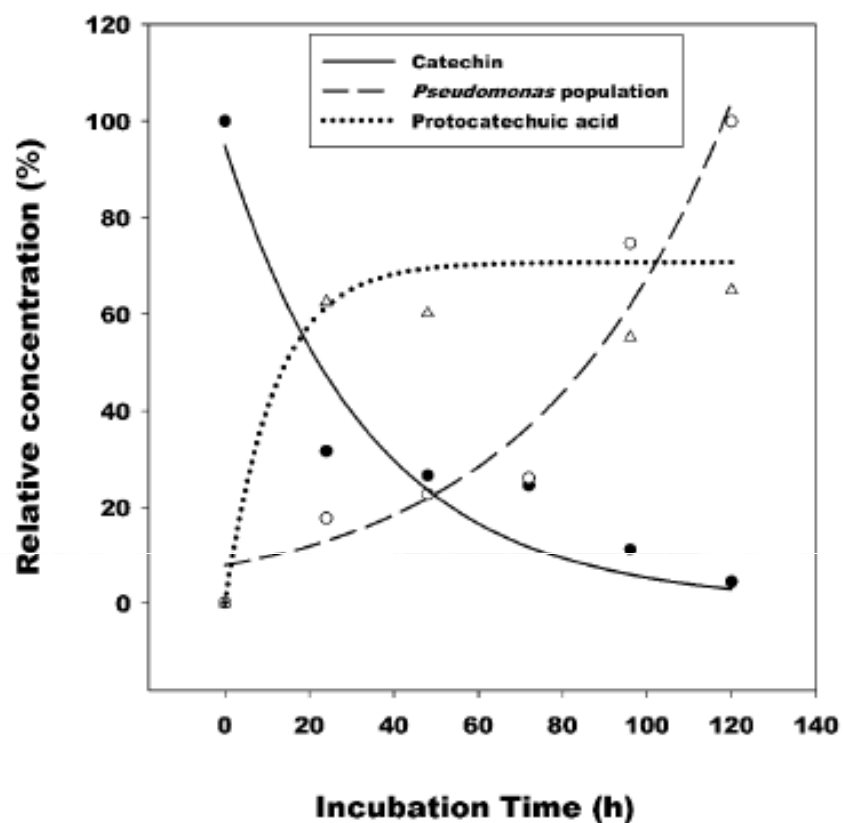
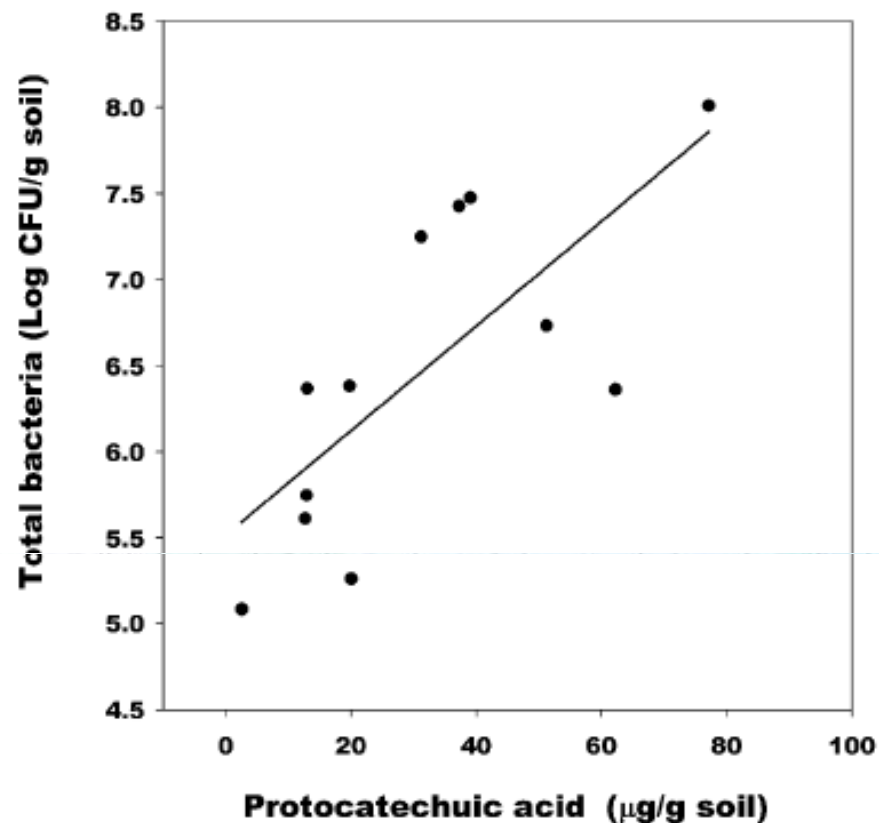




**Figure 3. Metabolic pathway for (-)-catechin transformed by *Pseudomonas* sp. CRF3-Ps-1 was analysed by the LC-ESI-MS/MS method (A).** (-)-Catechin (CAT) was transformed into taxifolin (Tax) via ketone formation during the first 24 h. Subsequently, C-ring hydrolysis occurred and generated protocatechuic acid (PCA) and glycerol (Gly). Finally, (-)-catechin was transformed into glycerol 72 h after incubation. The possible transformation hypothesis is also illustrated (B).

doi: 10.1371/journal.pone.0085162.g003



**(A)****(B)**

**Figure 4. Relative concentrations of (-)-catechin and protocatechuic acid, and the bacterial population in the medium, during 120 h incubation with *Pseudomonas* sp. CRF3-Ps-1**(A) (●) Relative concentration of catechin ( $r = -0.958$ ,  $P = 0.0025$ ,  $n = 6$ ); (○) Bacterial population of *Pseudomonas* CRF3-Ps-1 ( $r = 0.974$ ,  $P = 0.001$ ,  $n = 6$ ); (△) Relative concentration of protocatechuic acid ( $r = 0.874$ ,  $P = 0.0226$ ,  $n = 6$ ). (B) Correlations between the concentration of protocatechuic acid and bacterial populations in the soil of *R. formosanus* ( $r = 0.734$ ,  $P = 0.0066$ ,  $n = 12$ ).

doi: 10.1371/journal.pone.0085162.g004



**Table 1.** The concentration of allelochemicals in the soil of *Rhododendron formosanum* in Sunlinksea and Dasyueshan.

Study Site	Season	Catechin ( $\mu\text{g/g}$ soil)	Protocatechuic acid ( $\mu\text{g/g}$ soil)	Precipitation (mm/month)
Sunlinksea				
	Winter	5.30 $\pm$ 2.6	35.79 $\pm$ 2.3	35.67 $\pm$ 6.5
	Summer	178.36 $\pm$ 63.3*	14.07 $\pm$ 5.7*	199.77 $\pm$ 32.3**
	Typhoon	760	<1	635
Dasyueshan				
	Winter	6.94 $\pm$ 2.9	63.5 $\pm$ 7.5	27.37 $\pm$ 5.6
	Summer	237.44 $\pm$ 89.5	12.82 $\pm$ 0.1	224.93 $\pm$ 16.0***
	Typhoon	579	<1	726

Results are the mean  $\pm$  SE values of 3 experiments. Asterisks indicate significant difference (\* $p$  < 0.05, \*\* $p$  < 0.01, \*\*\* $p$  < 0.005) between seasons.

doi: 10.1371/journal.pone.0085162.t001



**Table 2.** The recovery value and half-life of standard (-)-catechin or protocatechuic acid in the soil from rhizosphere of *R. formosanum*.

Compound	(-)-Catechin	Protocatechuic acid
<b>Added concentration (<math>\mu\text{g/g}</math> soil)</b>	<b>200</b>	<b>25</b>
Measured mass concentration ( $\mu\text{g/g}$ soil)	$180.2 \pm 10.2$	$22.9 \pm 1.1$
Recovery (%)	90.1	91.5
RSD <sup>*</sup> (%)	5.0	4.4
Half-life in soil (hr)	$4.8 \pm 1.2$	>120

\* RSD: relative standard deviation

doi: 10.1371/journal.pone.0085162.t002



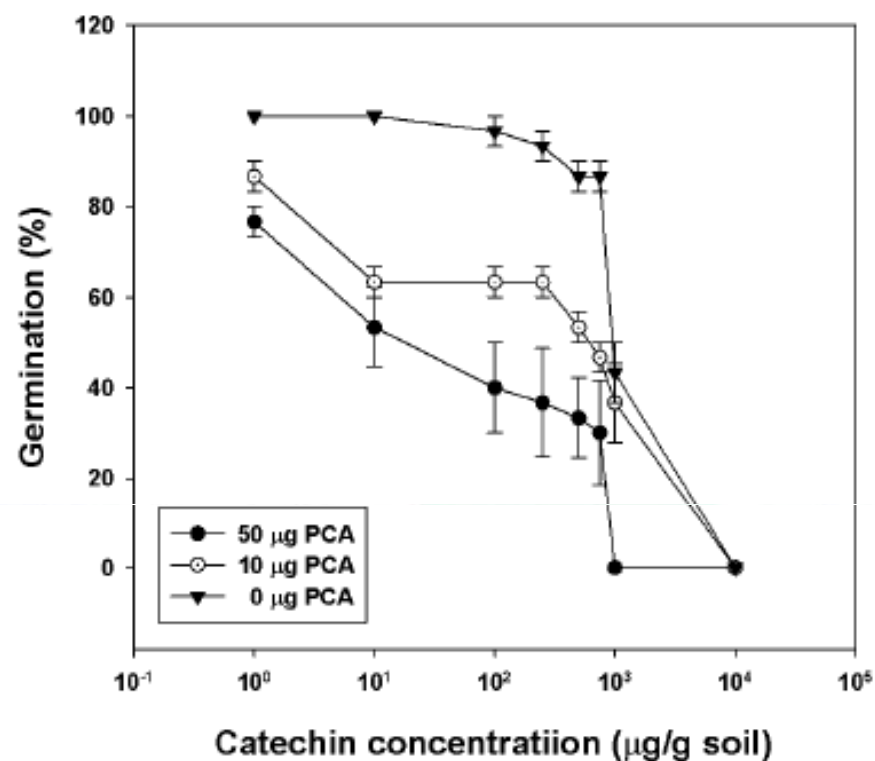
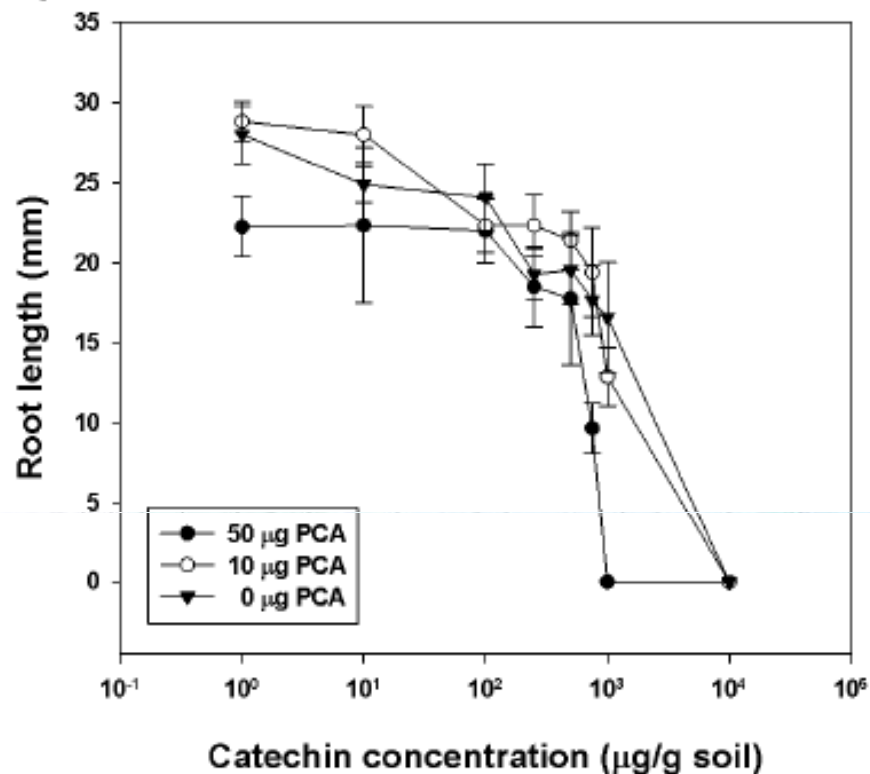
**Table 3.** Inhibitory effects of (-)-catechin and protocatechuic acid on the radicle length, germination, and  $ETR_{max}$  of *L. sativa* at the  $EC_{50}$  concentration.

	$EC_{50}$ (mM)		
	Radicle	Germination	$ETR_{max}$
(-)-Catechin	10.8 ± 1.8	9.2 ± 1.3	> 20
Protocatechuic acid	4.4 ± 0.3*	4.3 ± 0.4*	3.2 ± 0.03

Results are the mean ± SE values of 3 experiments. Asterisk indicates significant difference ( $p < 0.05$ ) between treatments.

doi: 10.1371/journal.pone.0085162.t003



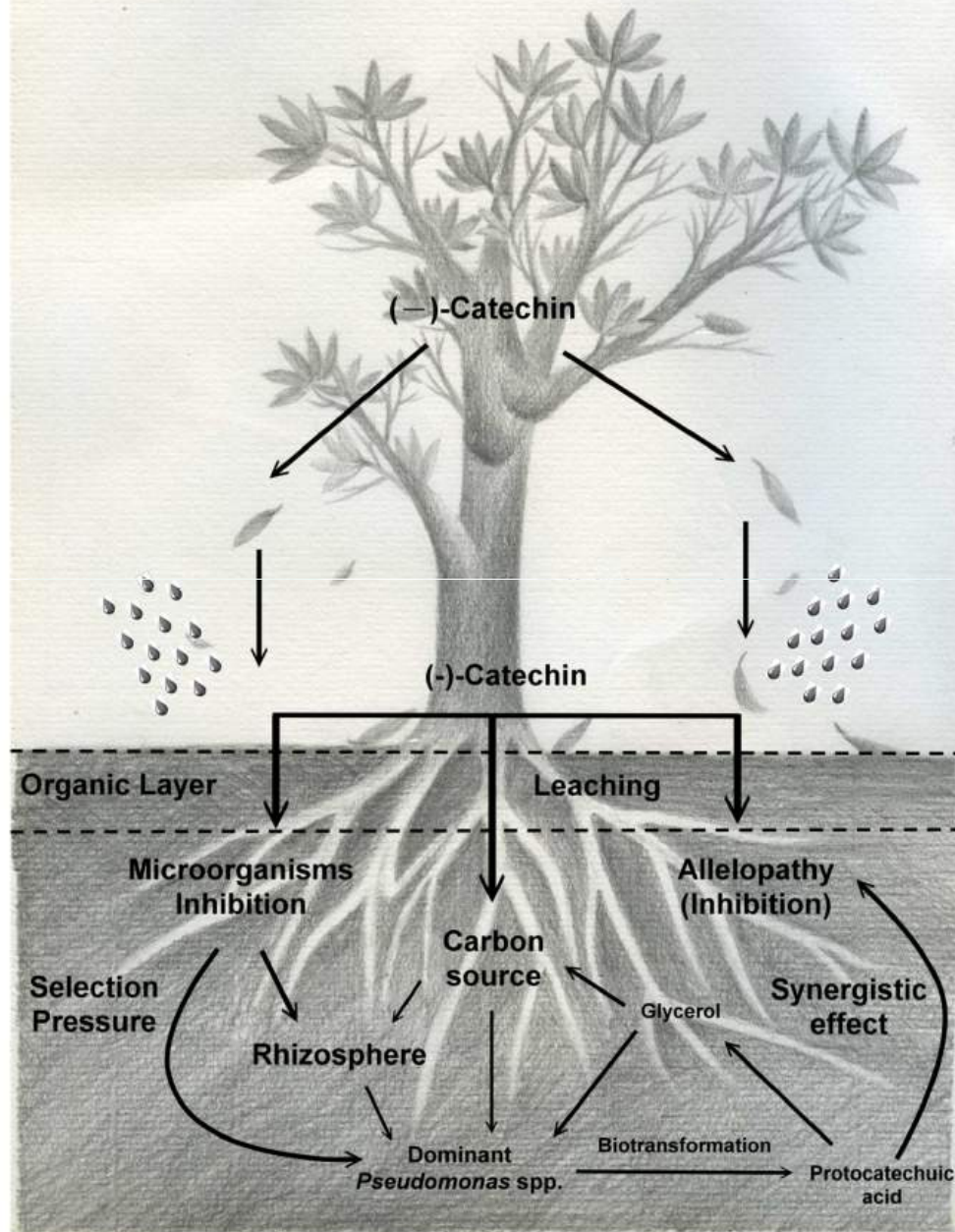
**(A)****(B)**

**Figure 5. The phytotoxic effects of (-)-catechin on the seed germination (A) and radicle growth (B) of *Lactuca sativa* at different concentrations in combination with 0 µg, 10 µg and 50 µg protocatechuic acid. Error bars represent the standard errors of the mean.**

doi: 10.1371/journal.pone.0085162.g005



*Rhododendron formosanum*



# Summary

- **Plants produce an array of chemicals and that many of these chemicals leach into the rhizosphere and have allelopathic effects on soil conditions, neighbouring plants, and microorganisms.**
- **Allelochemicals are utilized as nutrient sources and lead to an increase in the population of the selected microorganisms.**
- **Intermediate compounds of biotransformation have synergistic allelopathic effects with the original compounds**



# Plant Natural Products Can be Used as Pharmaceutical Agent

- **Anticancer**
- **Antioxidant**
- **Antibiotic**



## Chemical Constituents of *Rhododendron formosanum* Show Pronounced Growth Inhibitory Effect on Non-Small-Cell Lung Carcinoma Cells

Tzong-Der Way,<sup>†,§</sup> Shang-Jie Tsai,<sup>‡</sup> Chao-Min Wang,<sup>‡</sup> Chi-Tang Ho,<sup>⊗</sup> and Chang-Hung Chou<sup>\*,†,‡,⊥</sup>

<sup>†</sup>Department of Biological Science and Technology, College of Life Sciences, China Medical University, Taichung 40402, Taiwan

<sup>§</sup>Department of Health and Nutrition Biotechnology, College of Health Science, Asia University, Taichung 41354, Taiwan

<sup>‡</sup>Research Center for Biodiversity, China Medical University, Taichung 40402, Taiwan

<sup>⊗</sup>Department of Food Science, Rutgers University, New Brunswick, New Jersey 08901, United States

<sup>⊥</sup>Department of Biological Sciences, National Sun Yat-sen University, Kaohsiung 80424, Taiwan

# Lung cancer and Apoptosis

- **Lung cancer is the second most frequent type of cancer**
- **Nonsmall-cell lung cancer (NSCLC) accounts for ~80% of primary lung cancers**
- **Apoptosis, a major form of cell death, is regulated by programmed cellular signaling pathways**
- **Apoptosis is associated with characteristic morphological changes including the formation of apoptotic bodies, chromatin, and nuclear condensation and DNA fragmentation**



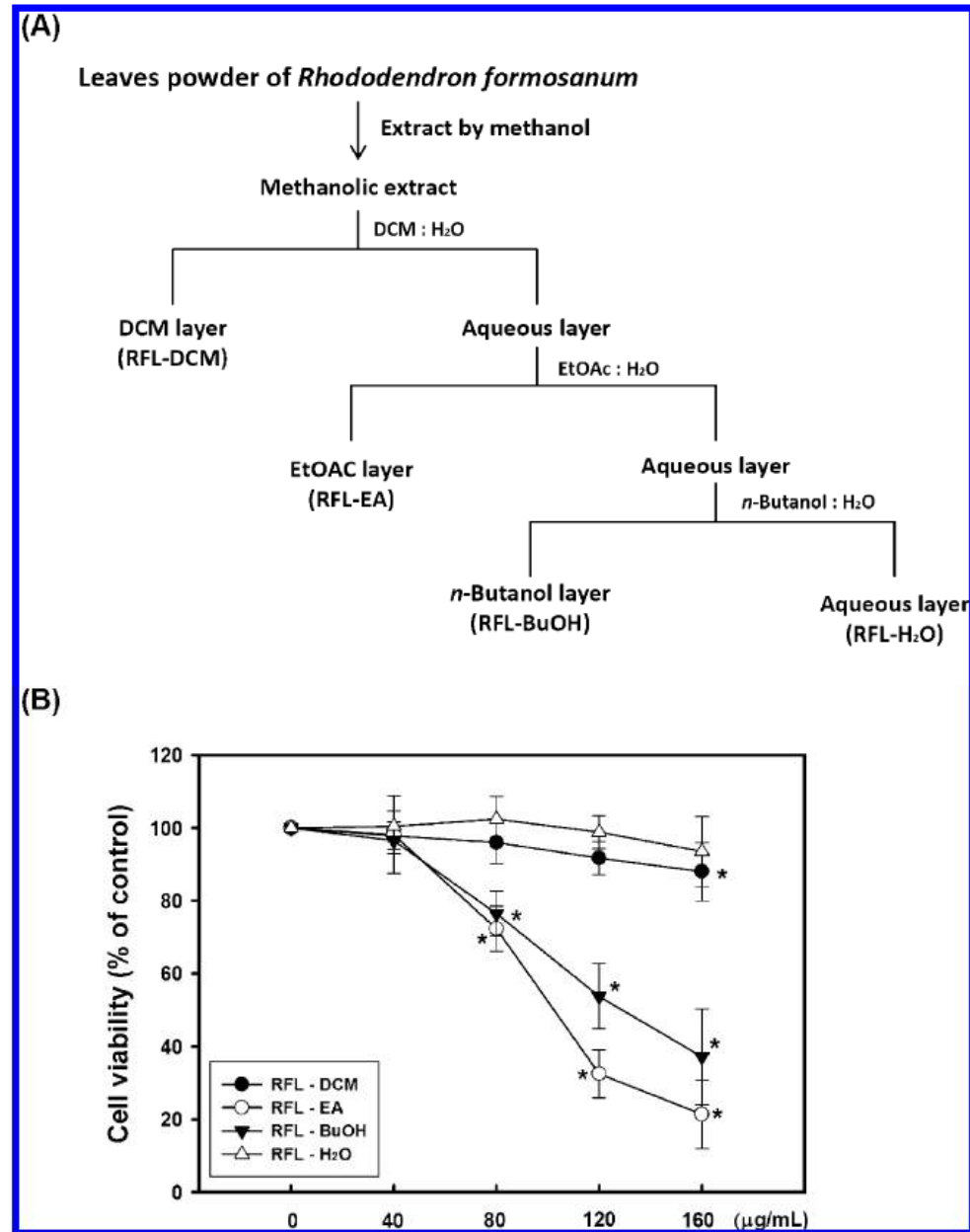


Figure 1. Antiproliferation activities of different fractions from *R. formosanum*. (A) Leaf powder of *R. formosanum* was extracted by methanol and partitioned into four fractions including dichloromethane, ethyl acetate, *n*-butanol, and water to get RFL-DCM, RFL-EA, RFL-BuOH, and RFL-H<sub>2</sub>O fractions. (B) A549 cells were treated with the four fractions (40–160 µg/mL) for 24 h. Cell viability was then determined using the MTT assay. This experiment was repeated three times. The data represent the mean ± SD. Values were significantly different from the control group: \*,  $P < 0.05$ .





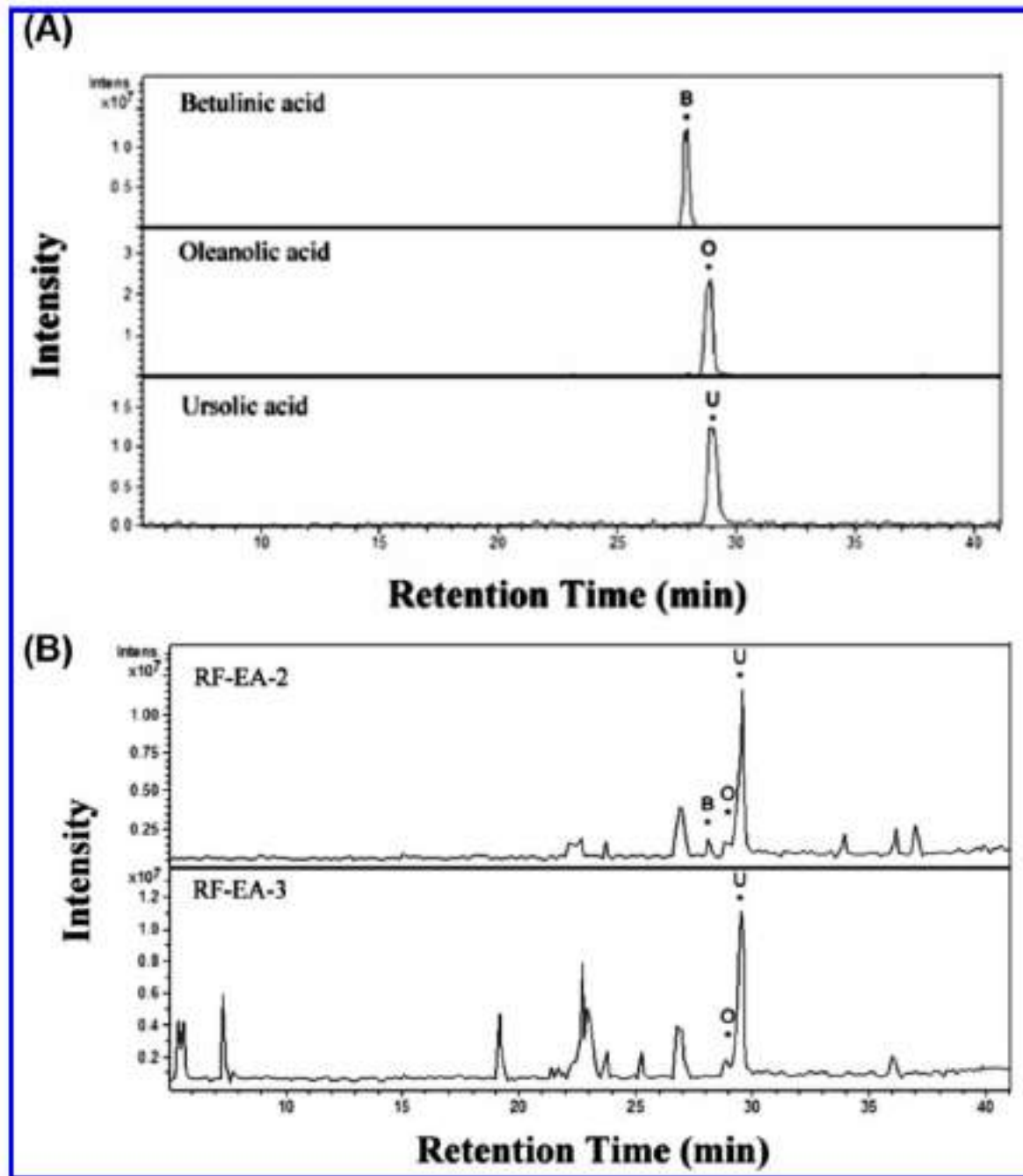


Figure 3. Quantification of triterpenoids by LC-ESI-MS/MS analysis. (A) Individual standard triterpenoids including betulinic acid (B), oleanolic acid (O), and ursolic acid (U) were subjected to LC-ESI-MS/MS analysis for chemical identification and quantification. Panel B shows quantification of the betulinic acid, oleanolic acid, and ursolic acid from RFL-EA-2 and RFL-EA-3 fractions.



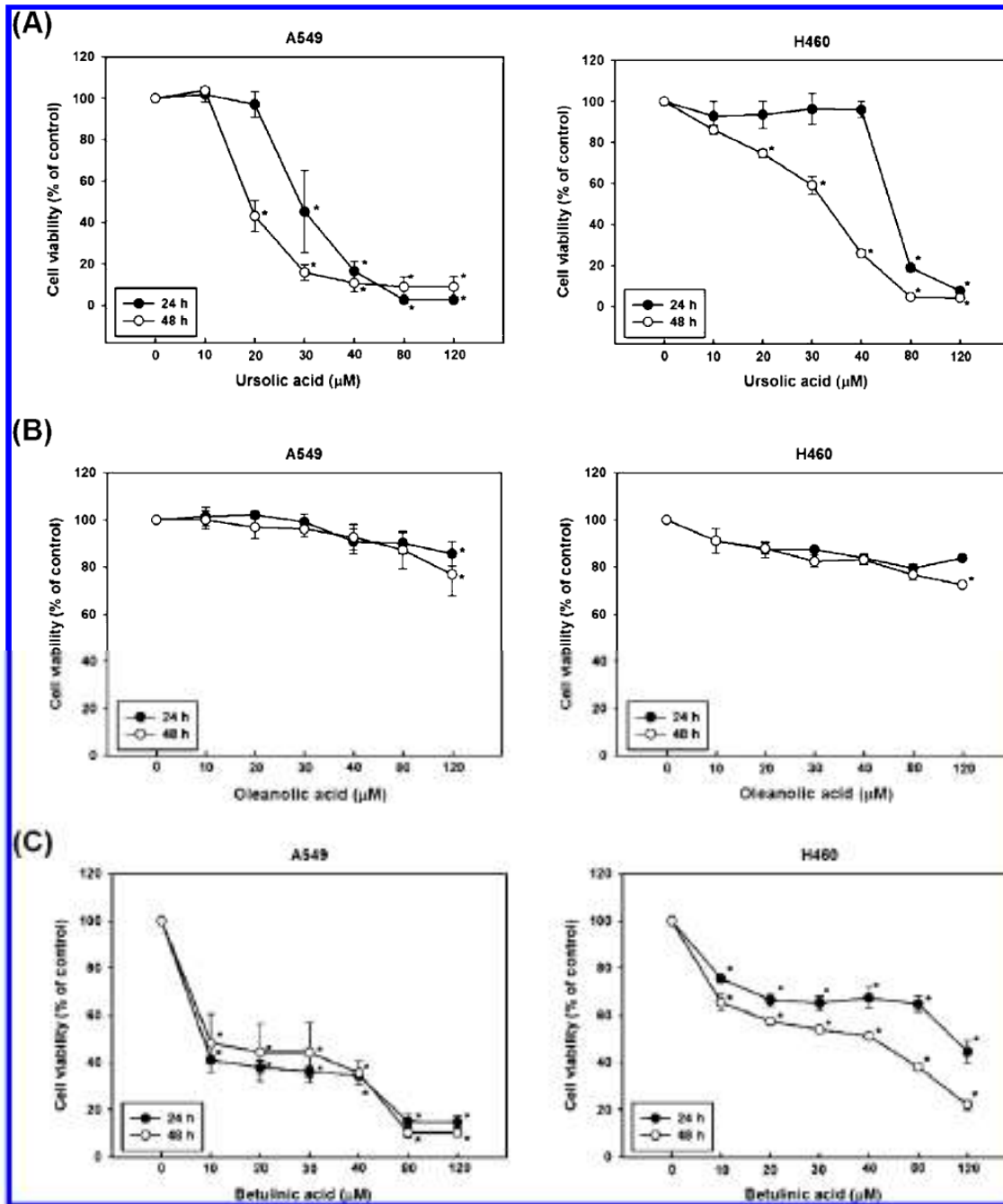


Figure 4. Antiproliferation effect of ursolic acid, oleanolic acid, and betulinic acid against NSCLC cells. A549 cells and H460 cells were treated with (A) ursolic acid, (B) oleanolic acid, and (C) betulinic acid at concentrations of 10–160  $\mu\text{M}$  for 24 or 48 h. Cell viability was then determined using the MTT assay. This experiment was repeated three times. The data represent the mean  $\pm$  SD. Values were significantly different from the control groups \*,  $P < 0.05$ .



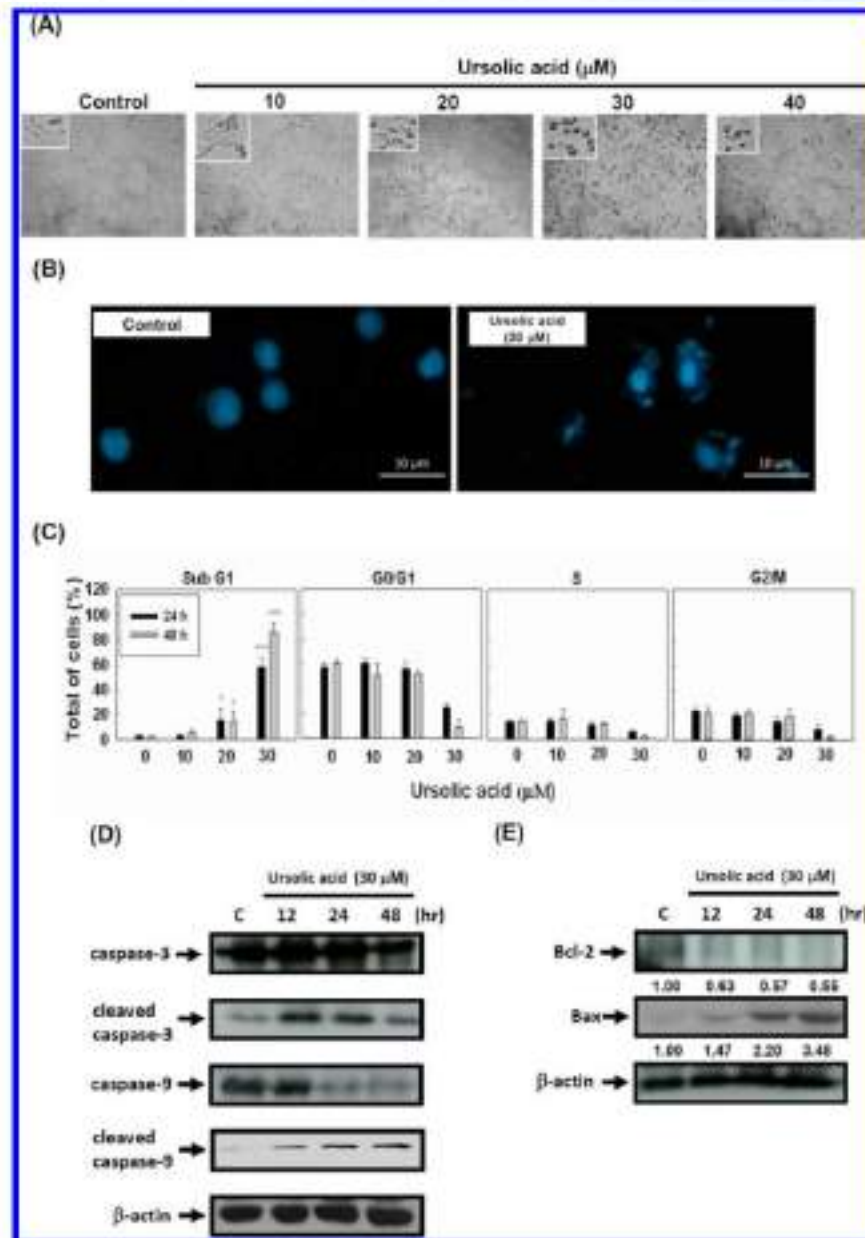
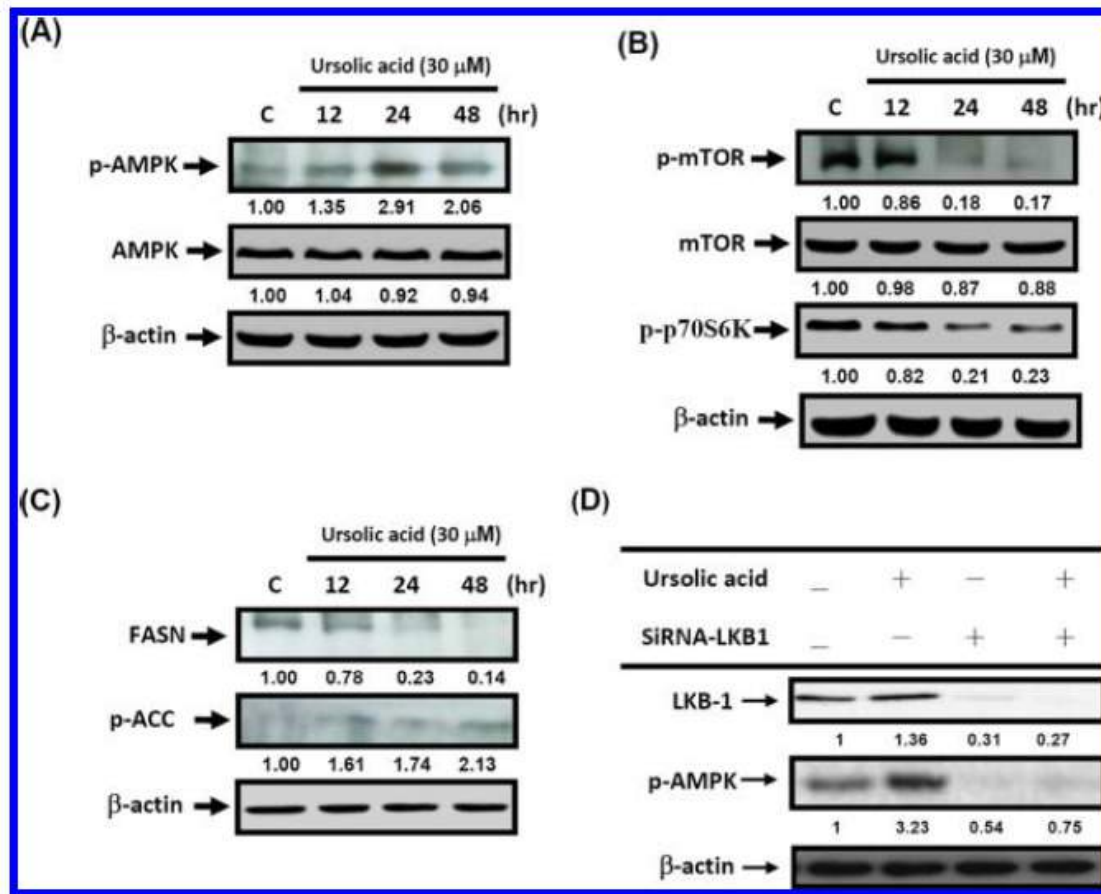


Figure 5. Ursolic acid induced A549 cell apoptosis. (A) A549 cells were incubated with ursolic acid (10–40  $\mu\text{M}$ ) for 24 h, and morphology was observed by photomicroscope. (B) the morphology of cell nuclei was observed by fluorescence microscope. (C) To observe cell cycle statements and apoptosis levels, cell were stained with PI and measured by flow cytometry. (D) A549 cells were treated with ursolic acid (30  $\mu\text{M}$ ) for the indicated time. Cells were then harvested and lysed for the detection of caspase-3, cleaved caspase-3, caspase-9, cleaved caspase-9, and  $\beta$ -actin. (E) A549 cells were treated with ursolic acid (30  $\mu\text{M}$ ) for the indicated times. Cells were then harvested and lysed for the detection of Bcl-2, Bax, and  $\beta$ -actin. Western blot data presented are representative of those obtained in at least three separate experiments. The values below the figures represent change in protein expression of the bands normalized to  $\beta$ -actin.



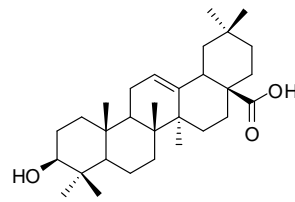
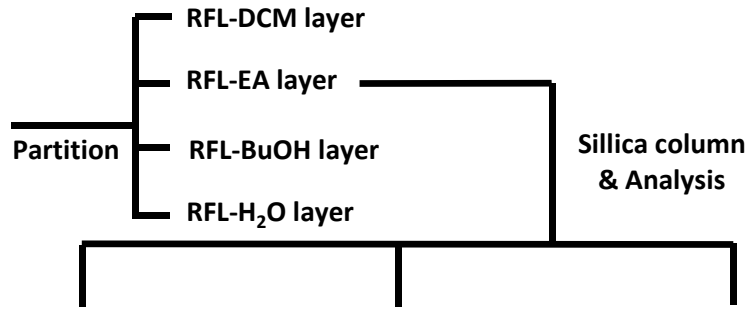


**Figure 6.** Ursolic acid decreases general mRNA translation and the activity of fatty acid synthesis via activation of AMPK. (A) A549 cells were treated with ursolic acid (30  $\mu$ M) for the indicated times. Cells were then harvested and lysed for the detection of phosphorylated AMPK (Thr 172), AMPK, and  $\beta$ -actin. (B) A549 cells were treated with ursolic acid (30  $\mu$ M) for the indicated times. Cells were then harvested and lysed for the detection of phosphorylated mTOR (Ser 2448), mTOR, phosphorylated p70S6K, and  $\beta$ -actin. (C) A549 cells were treated with ursolic acid (30  $\mu$ M) for the indicated times. Cells were then harvested and lysed for the detection of FASN, phospho-ACC (Ser79), and  $\beta$ -actin. (D) A549 cells were transfected with 50 nmol/L LKB1-siRNA using Oligofectamine. A total of 24 h after transfection, cells were treated with ursolic acid (30  $\mu$ M) for 24 h. After harvesting, cells were lysed and prepared for Western blotting analysis using antibodies against LKB-1, phosphorylated AMPK (Thr 172), and  $\beta$ -actin. Western blot data presented are representative of those obtained in at least three separate experiments. The values below the figures represent change in protein expression of the bands normalized to  $\beta$ -actin.

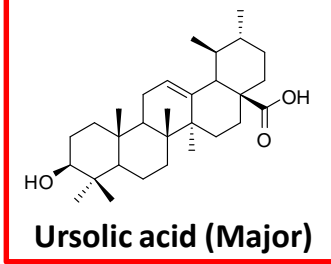




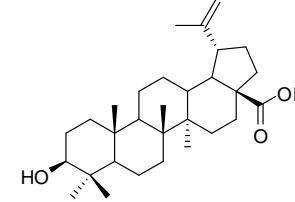
*Rhododendron formosanum* leaves



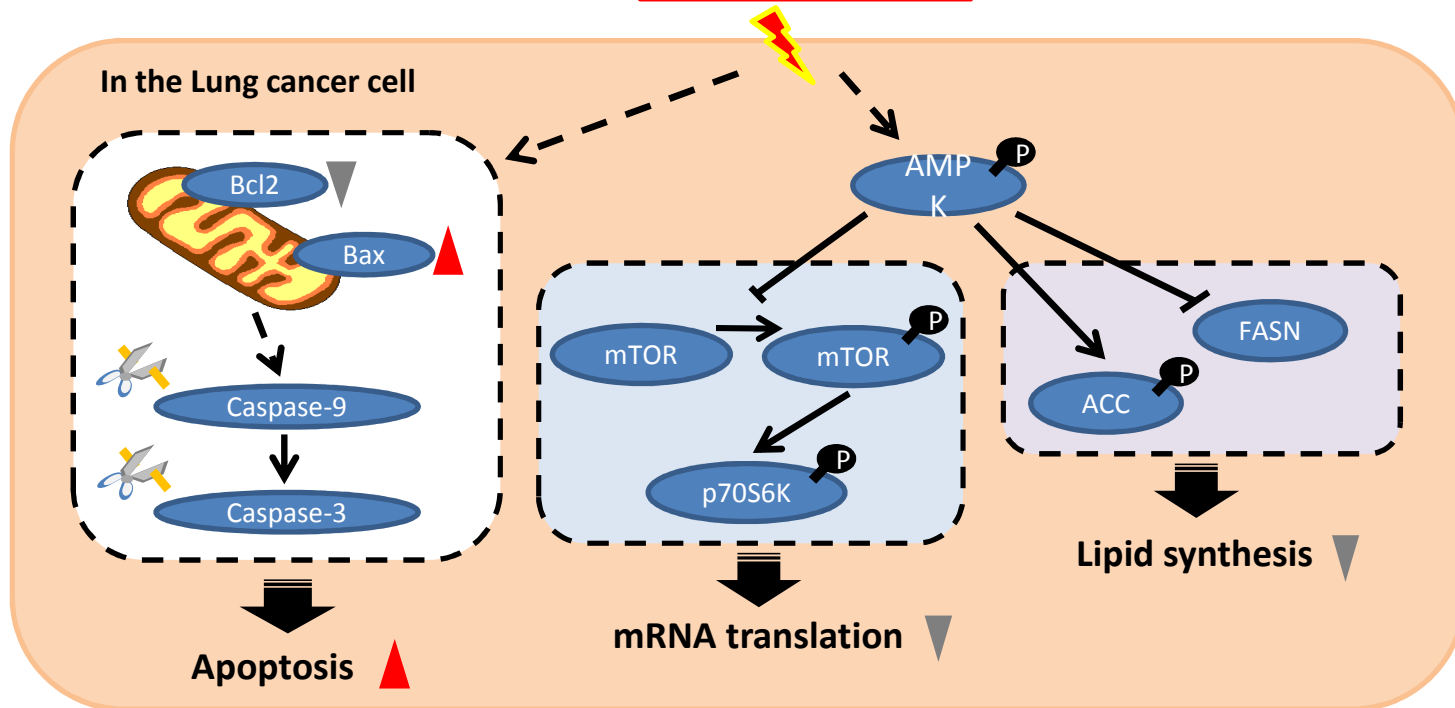
Oleanolic acid



Ursolic acid (Major)



Betulinic acid



*Article*

## Structure Elucidation of Procyanidins Isolated from *Rhododendron formosanum* and Their Anti-Oxidative and Anti-Bacterial Activities

Chao-Min Wang <sup>1</sup>, Yuan-Man Hsu <sup>2</sup>, Yun-Lian Jhan <sup>1</sup>, Shang-Jie Tsai <sup>1</sup>, Shi-Xun Lin <sup>1</sup>, Chiu-Hsian Su <sup>2</sup> and Chang-Hung Chou <sup>1,2,3,\*</sup>

<sup>1</sup> Research Center for Biodiversity, China Medical University, Taichung 40402, Taiwan; E-Mails: wangchaomin@mail.cmu.edu.tw (C.-M.W.); ah\_giu@hotmail.com (Y.-L.J.); csungjay@yahoo.com.tw (S.-J.T.); flyalonewithme9147@gmail.com (S.-X.L.)

<sup>2</sup> Department of Biological Science and Technology, China Medical University, Taichung 40402, Taiwan; E-Mails: yuanmh@mail.cmu.edu.tw (Y.-M.H.); adaga0806@hotmail.com (C.-H.S.)

<sup>3</sup> Department of Life Sciences, National Cheng Kung University, Tainan 701, Taiwan



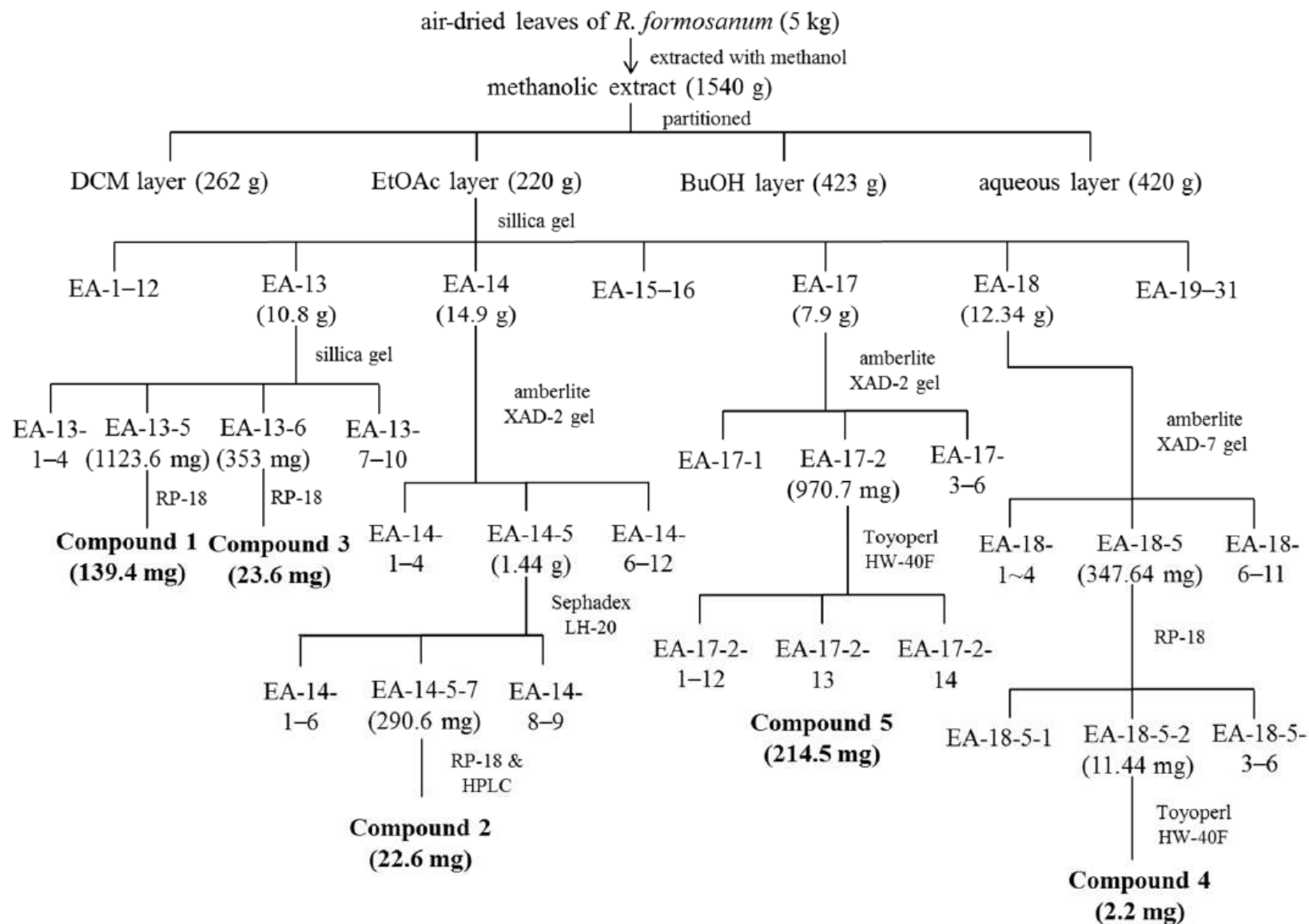
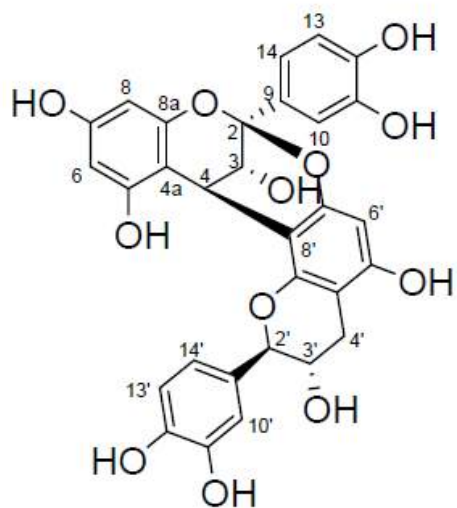
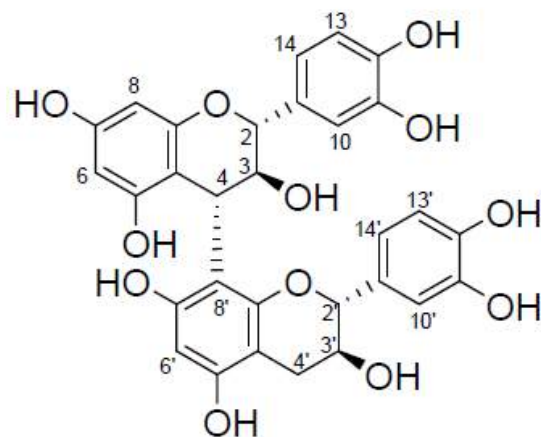


**Figure 5.** Purification flow chart of procyanidins isolated from *R. formosanum*.

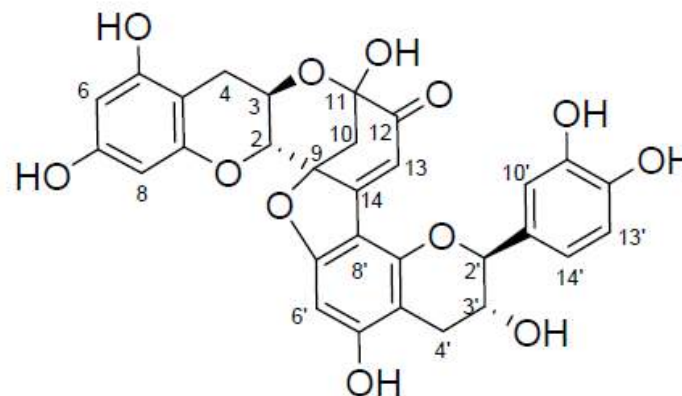




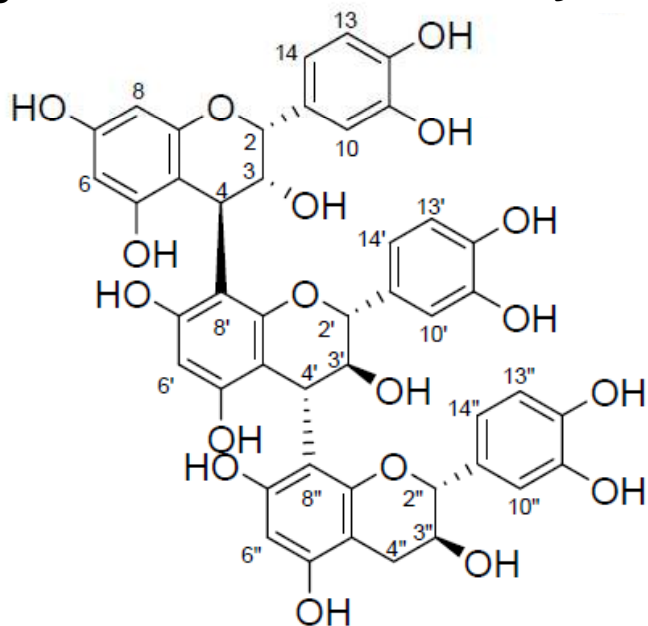
**Procyanidin A1**



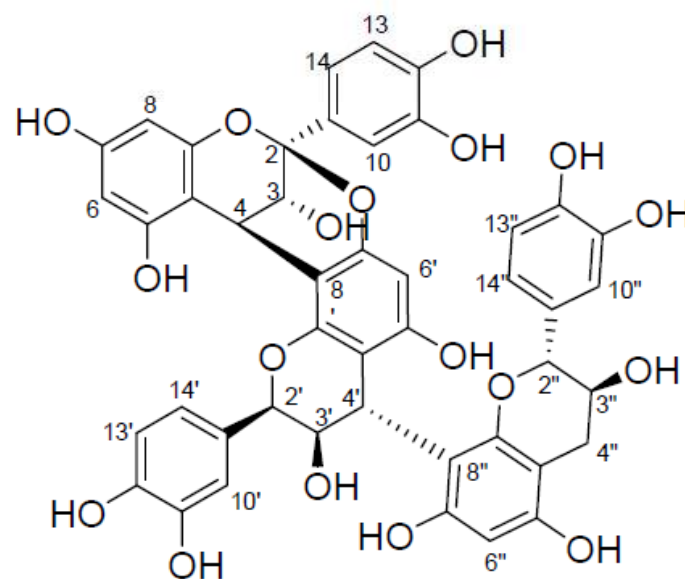
**Procyanidin B3**



**Rhodonidin A**



**Procyanidin C4**



**Cinnamtannin D1**

**Figure 1.** Chemical structure of procyanidines from *R. formosanum*

**Table 2.** The minimum inhibitory concentration ( $\mu\text{g/mL}$ ) of antibiotics and natural procyanidins for different bacterial pathogens.

Pathogens	Minimum Inhibitory Concentration ( $\mu\text{g/mL}$ )							
	Antibiotics and Procyanidins							
	Ap *	Tet	Met	1	2	3	4	5
<i>Staphylococcus aureus</i>	16	8	<sup>†</sup> N.D.	64	64	4	>128	>128
<i>Enterococcus faecalis</i>	2	4	N.D.	>128	>128	>128	>128	>128
<i>Listeria monocytogenes</i>	1	2	N.D.	64	>128	>128	>128	>128
<i>Bacillus cereus</i>	128	4	N.D.	64	>128	>128	>128	>128
<i>Escherichia coli</i>	4	0.5	N.D.	>128	>128	>128	>128	>128
<i>Salmonella enterica</i>	1	8	N.D.	>128	>128	>128	>128	>128
<i>Pseudomonas aeruginosa</i>	512	32	N.D.	>128	>128	>128	>128	>128
<i>Helicobacter pylori</i> **	N.D.	N.D.	2	>256	>256	>256	>256	>256

\* Ap: ampicillin; Tet: tetracycline; Met: metronidazole; **1**: procyanidin A1; **2**: procyanidin B3; **3**: rhodonidin A; **4**: procyanidin C4; **5**: cinnamtannin D1; \*\* *H. pylori* was tested by minimum bactericidal concentration method.

<sup>†</sup>N.D.: not determined.



**Table 3.** The antioxidant activities of the procyanidins from leaves of *R. formosanum* using the DPPH free radical-scavenging assay ( $IC_{50}$ ,  $\mu M$ ) and CUPric reducing antioxidant capacity (CUPRAC) method (TEACs).

Compounds	Total OH Groups	Average OH/unit	Antioxidant Activity	
			$IC_{50}/DPPH$ ( $\mu g/mL$ )	CUPRAC (TEACs)
Trolox	2	2	61.12	1.00
(-)-Catechin	5	5	27.07	2.74
<b>1</b>	9	4.5	20.89	1.75
<b>2</b>	10	5	8.55	4.87
<b>3</b>	7	3.5	13.06	1.96
<b>4</b>	15	5	6.26	3.48
<b>5</b>	14	4.7	3.29	2.93



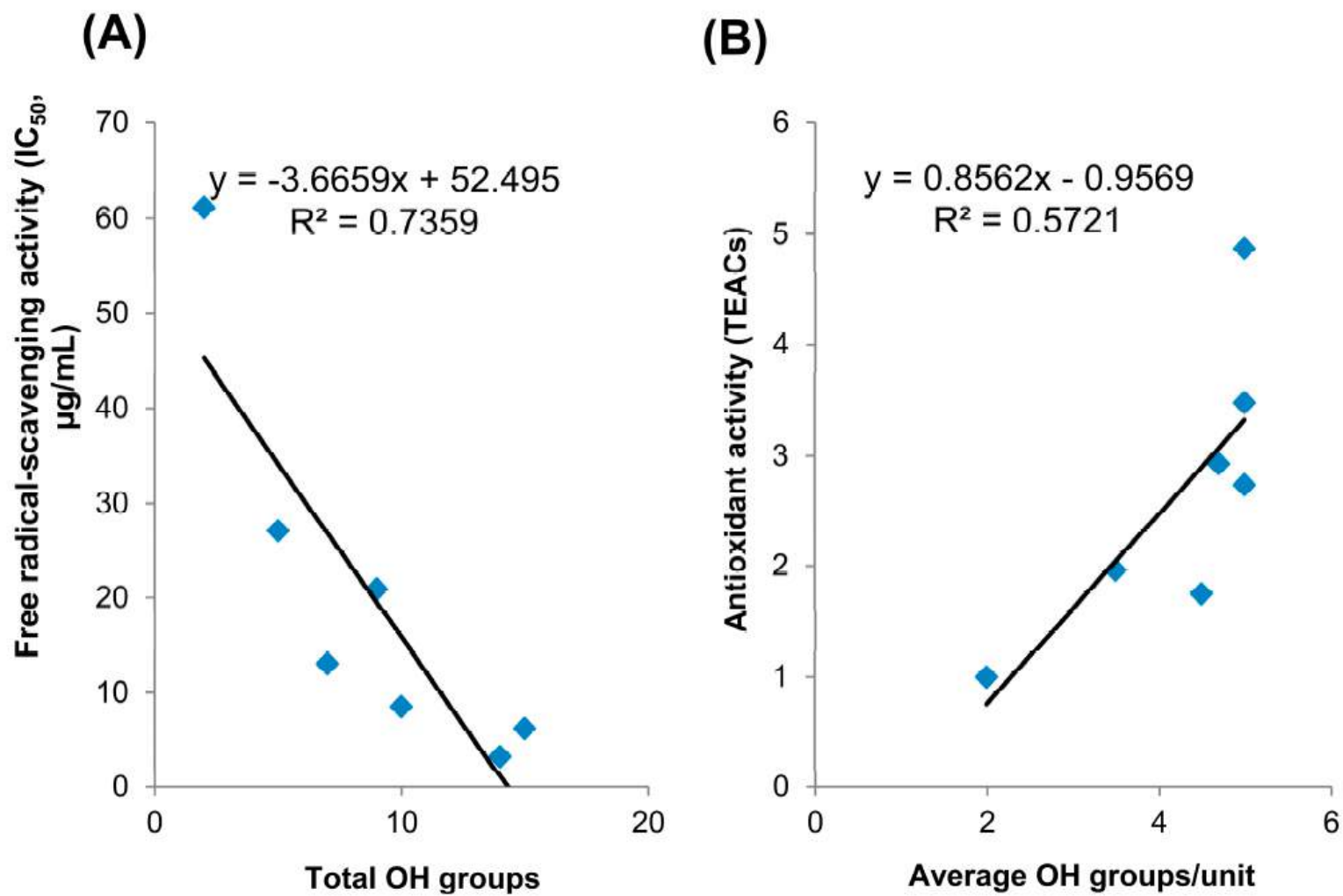


**Figure 4.** Correlations of total OH groups with free radical-scavenging activity (A) and average OH groups/unit with antioxidant activity (B).



# Cinnamtannin D1 from *Rhododendron formosanum* Induces Autophagy via the Inhibition of Akt/mTOR and Activation of ERK1/2 in Non-Small-Cell Lung Carcinoma Cells

Tzong-Der Way,<sup>†,§</sup> Shang-Jie Tsai,<sup>‡</sup> Chao-Min Wang,<sup>‡</sup> Yun-Lian Jhan,<sup>‡</sup> Chi-Tang Ho,<sup>||</sup>  
and Chang-Hung Chou<sup>\*,†,‡,⊥</sup>

<sup>†</sup>Department of Biological Science and Technology, College of Biopharmaceutical and Food Sciences, and <sup>‡</sup>Research Center for Biodiversity, China Medical University, Taichung 40402, Taiwan

<sup>§</sup>Department of Health and Nutrition Biotechnology, College of Health Science, Asia University, Taichung 41354, Taiwan

<sup>||</sup>Department of Food Science, Rutgers University, New Brunswick, New Jersey United States

<sup>⊥</sup>Department of Life Sciences, National Cheng Kung University, Tainan 701, Taiwan

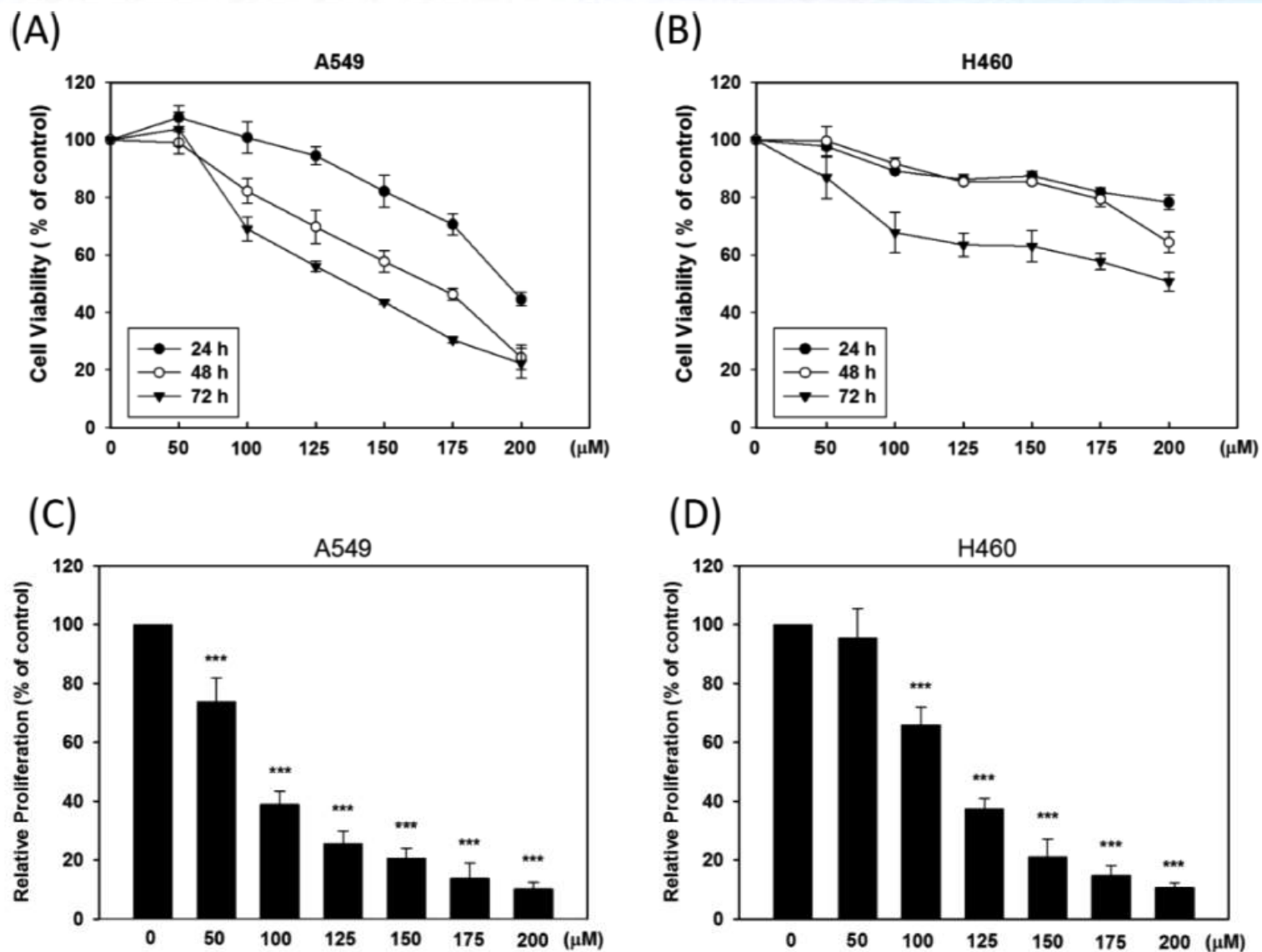


Figure 2. Effect of CNT D1 on antiproliferation activity. (A) A549 and (B) H460 cells were treated with CNT D1 at different concentrations for 24, 48, and 72 h and measured by the MTT assay. After (C) A549 and (D) H460 cells were treated with CNT D1 for 72 h, the cell proliferation ability of A549 and H460 cells was measured by the BrdU cell proliferation assay. These experiments were repeated three times. The data represent the mean  $\pm$  SD.



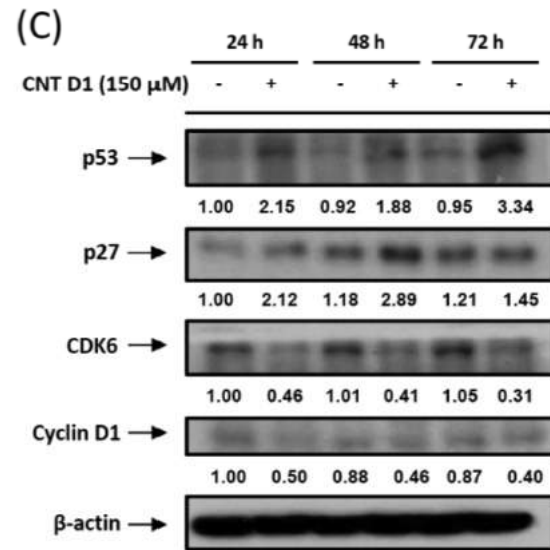
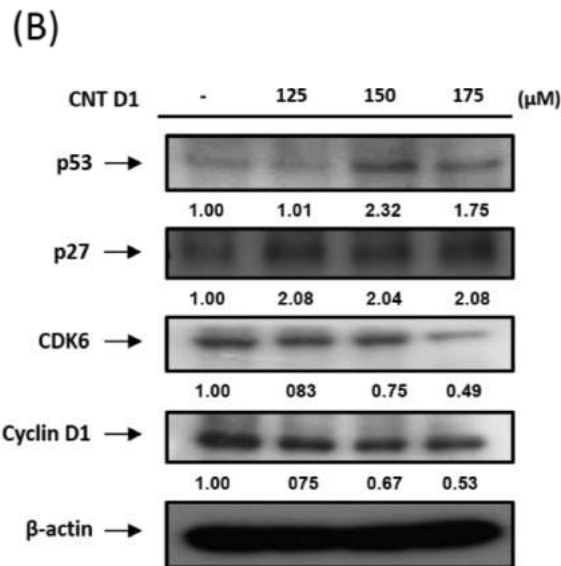
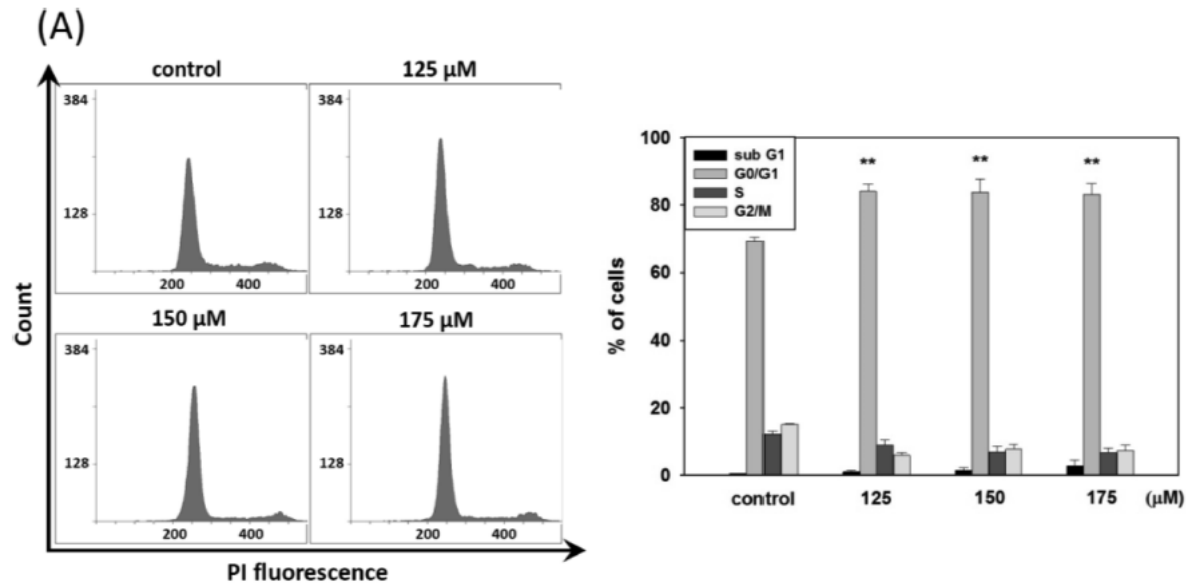
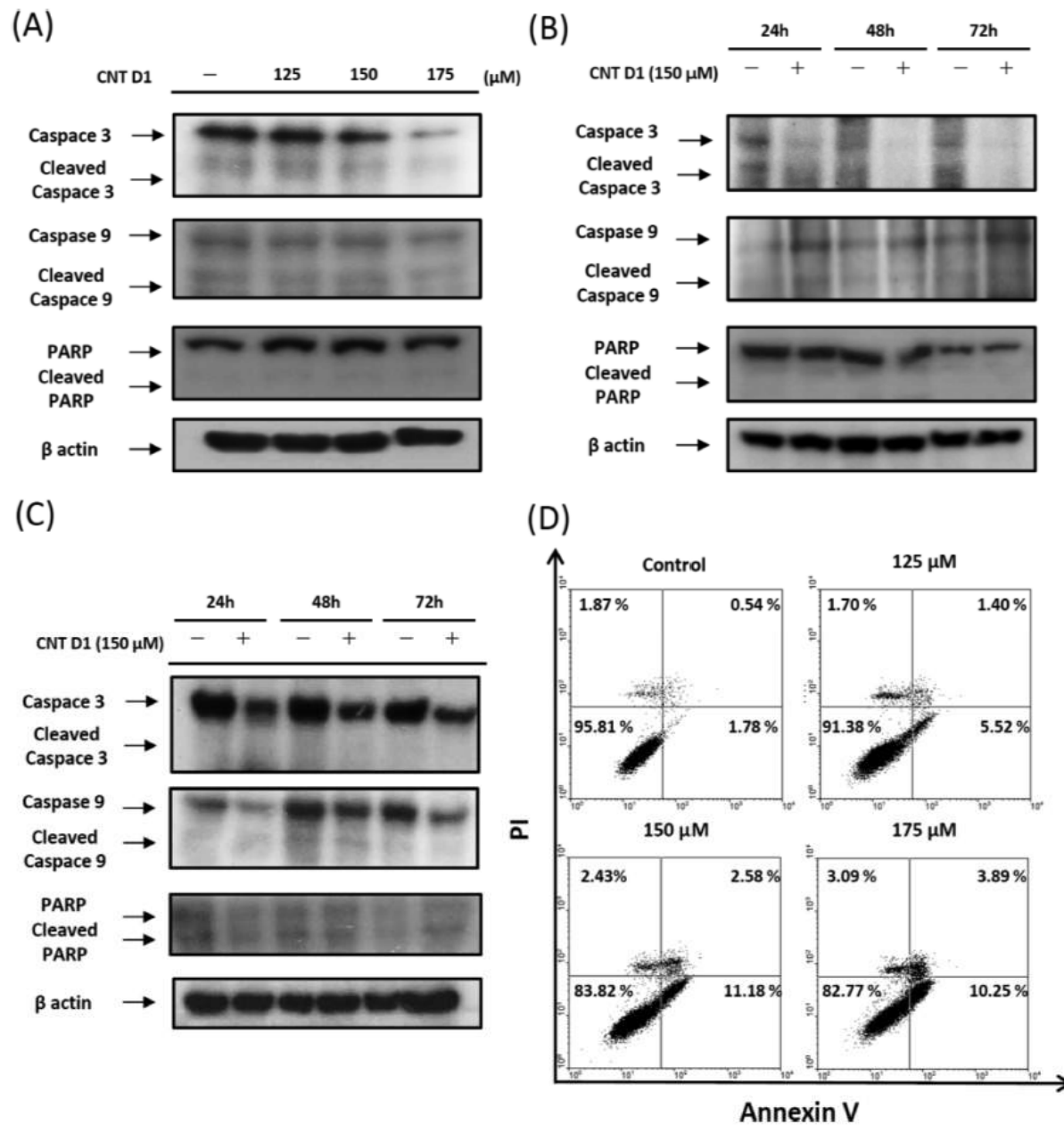


Figure 3. Effect of CNT D1 on cell cycle distribution and related protein expression. (A) To observe the state of the cell cycle, A549 cells were treated with CNT D1 at 125, 150, and 175 μM for 72 h. Cells were stained with PI and measured by flow cytometry. Results are described as means ± SD, and the statistical significance between the control group and different experimental groups is presented with asterisks (\*,  $P < 0.05$ ; \*\*,  $P < 0.005$ ; \*\*\*,  $P < 0.001$ ). (B) A549 cells were treated with CNT D1 at 125, 150, and 175 μM for 72 h. (C) A549 cells were treated with CNT D1 (150 μM) for the indicated time. The protein expression of p53, p27, CDK6, and cyclin D1 was measured by Western blot. Western blot data presented are representative of those obtained in at least three separate experiments. The values below the figures represent the change in protein expression of the bands normalized to β-actin.





**Figure 4.** Effect of CNT D1 on cleavage of caspase 3, caspase 9, and PARP. (A) A549 cells treated with CNT D1 at 125, 150, and 175  $\mu$ M for 72 h. (B) A549 and (C) H460 cells were treated with CNT D1 (150  $\mu$ M) for the indicated time. The protein expression of caspase 3, cleaved caspase 3, caspase 9, cleaved caspase 9, PARP, and cleaved PARP were measured by Western blot. Western blot data presented are representative of those obtained in at least three separate experiments. The values below the figures represent the change in protein expression of the bands normalized to  $\beta$ -actin. (D) After A549 cells were treated with CNT D1 for 72 h, cells were stained with annexin V-FITC and PI and measured by flow cytometry.



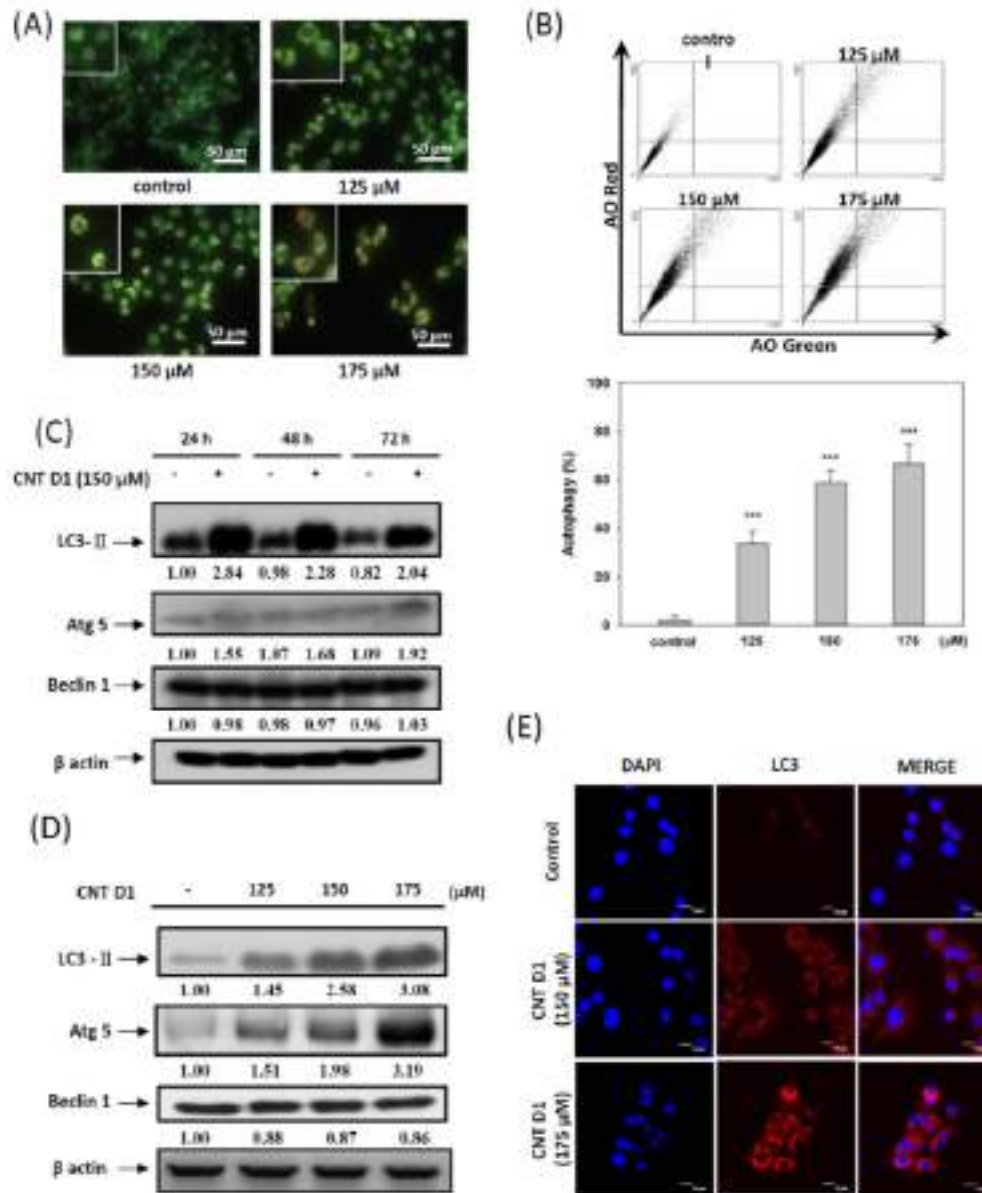
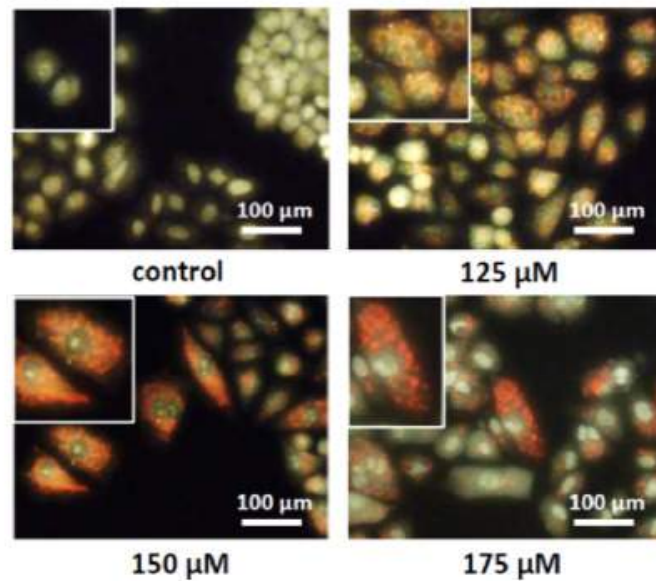


**Figure 5.** CNT D1-induced autophagy in A549 Cells. (A) A549 cells treated with CNT D1 at 125, 150, and 175  $\mu\text{M}$  for 72 h and stained with AO. The autophagy of cell morphology was observed by fluorescence microscopy. Scale bar: 50  $\mu\text{m}$ . (B) The AO-stained acidic vacuoles on CNT D1-treated A549 cells were measured by flow cytometry. Scale bar: 50  $\mu\text{m}$ . Autophagy data are described as means  $\pm$  SD, and the statistical significance between the control group and different experimental groups is presented with asterisks (\*,  $P < 0.05$ ; \*\*,  $P < 0.005$ ; \*\*\*,  $P < 0.001$ ). (C) A549 cells treated with CNT D1 at 125, 150, and 175  $\mu\text{M}$  for 72 h. (D) A549 cells were treated with CNT D1 (150  $\mu\text{M}$ ) for the indicated time. The protein expression of LC3 II, Atg 5, and Beclin 1 were measured by Western blot. Western blot data presented are representative of those obtained in at least three separate experiments. The values below the figures represent the change in protein expression of the bands normalized to  $\beta$ -actin. (E) Detecting the LC3 accumulation by immunofluorescence. A549 cells were stained with rabbit monoclonal anti-LC3 and PE-conjugated secondary antibodies (red), and nuclei were stained with DAPI (blue). Results were observed by confocal microscope. Scale bar: 10  $\mu\text{m}$ .



(A)



(B)

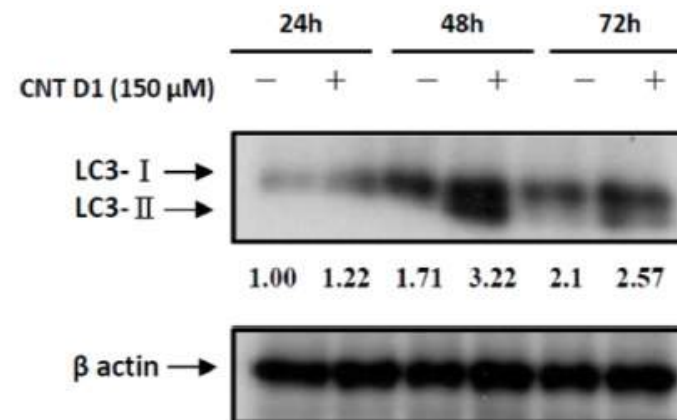
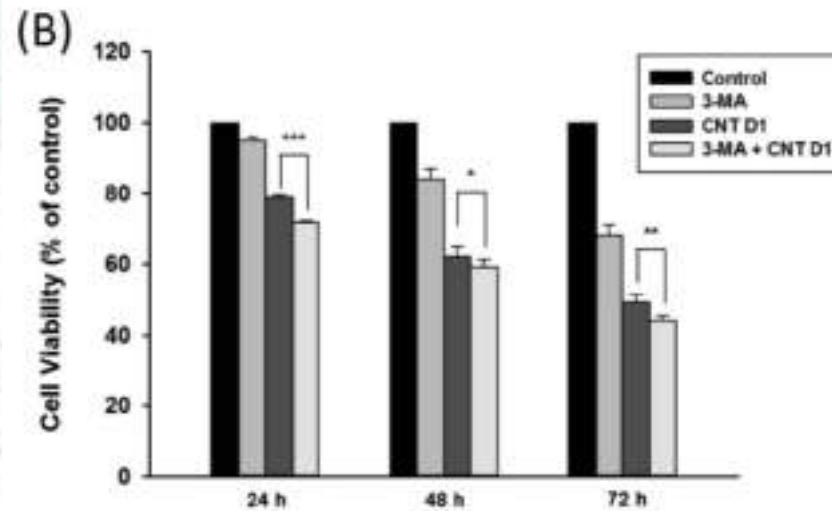
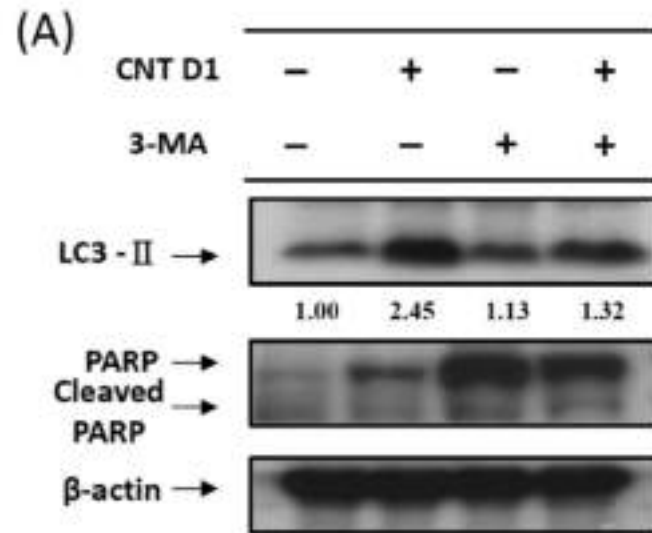


Figure 6. CNT D1-induced autophagy in H460 cells. (A) H460 cells treated with CNT D1 at 125, 150, and 175  $\mu$ M for 72 h and stained with AO. The autophagy of cell morphology was observed by fluorescence microscopy. Scale bar: 100  $\mu$ m. (B) H460 cells were treated with CNT D1 (150  $\mu$ M) for the indicated time. The protein expression of LC3 II was measured by Western blot. Western blot data presented are representative of those obtained in at least three separate experiments. The values below the figures represent change in protein expression of the bands normalized to  $\beta$ -actin.





**Figure 7.** Autophagy inhibition by 3-MA. After A549 cells were pretreated with 1 mM 3-MA for 1 h, they were cotreated with 150  $\mu$ M CNT D1 and 1 mM 3-MA for 72 h. (A) Protein expression of LC3 I, LC3 II, PARP, and cleaved PARP was determined by Western blot. (B) Cell viability was measured by MTT assay. Results are described as means  $\pm$  SD, and between the CNT D1 group and 3-MA + CNT D1 group, the statistical significance is presented with asterisks (\*,  $P < 0.05$ ; \*\*,  $P < 0.005$ ; \*\*\*,  $P < 0.001$ ).



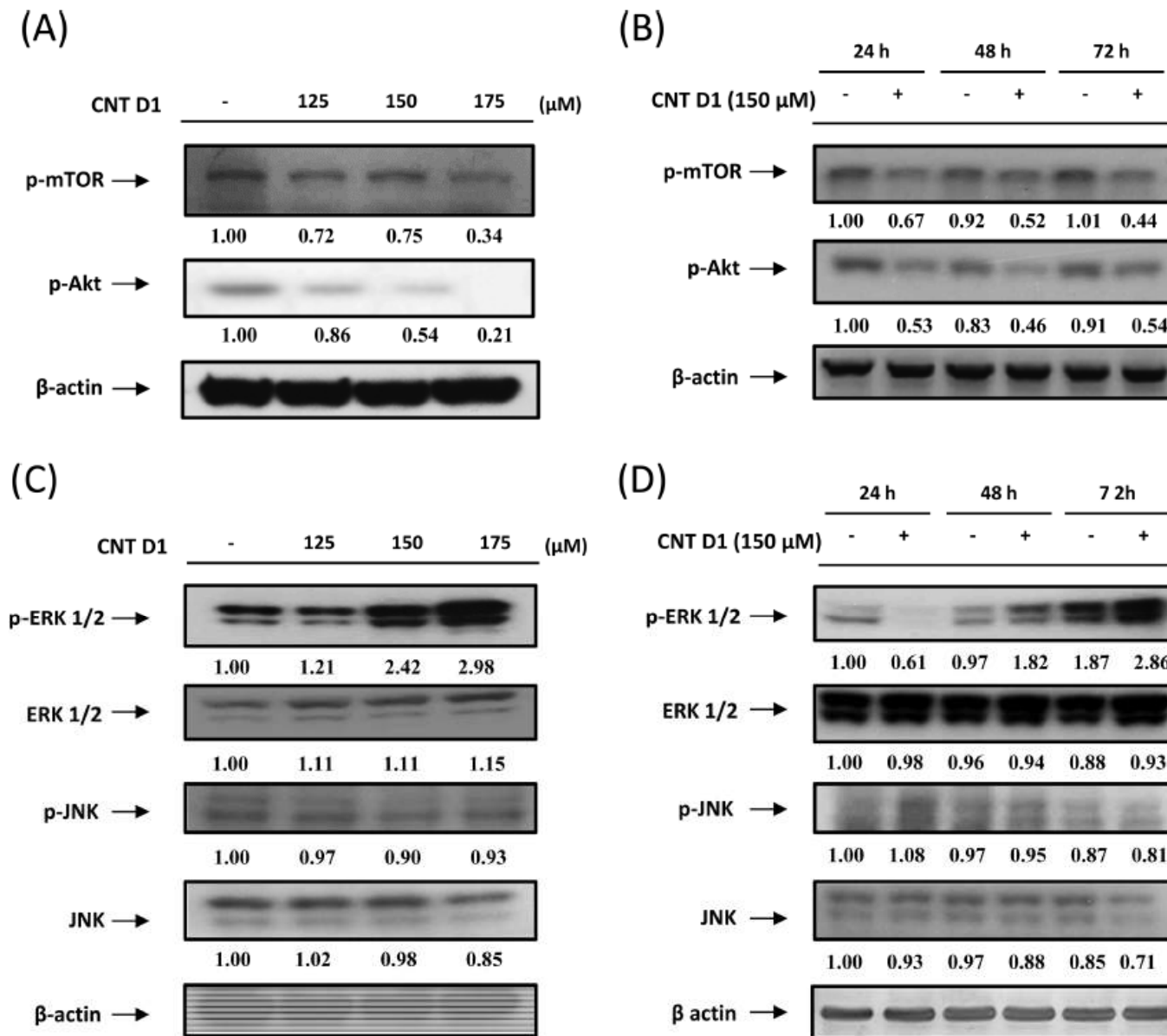
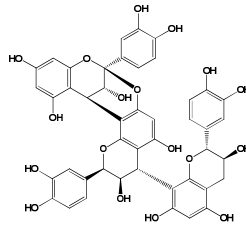
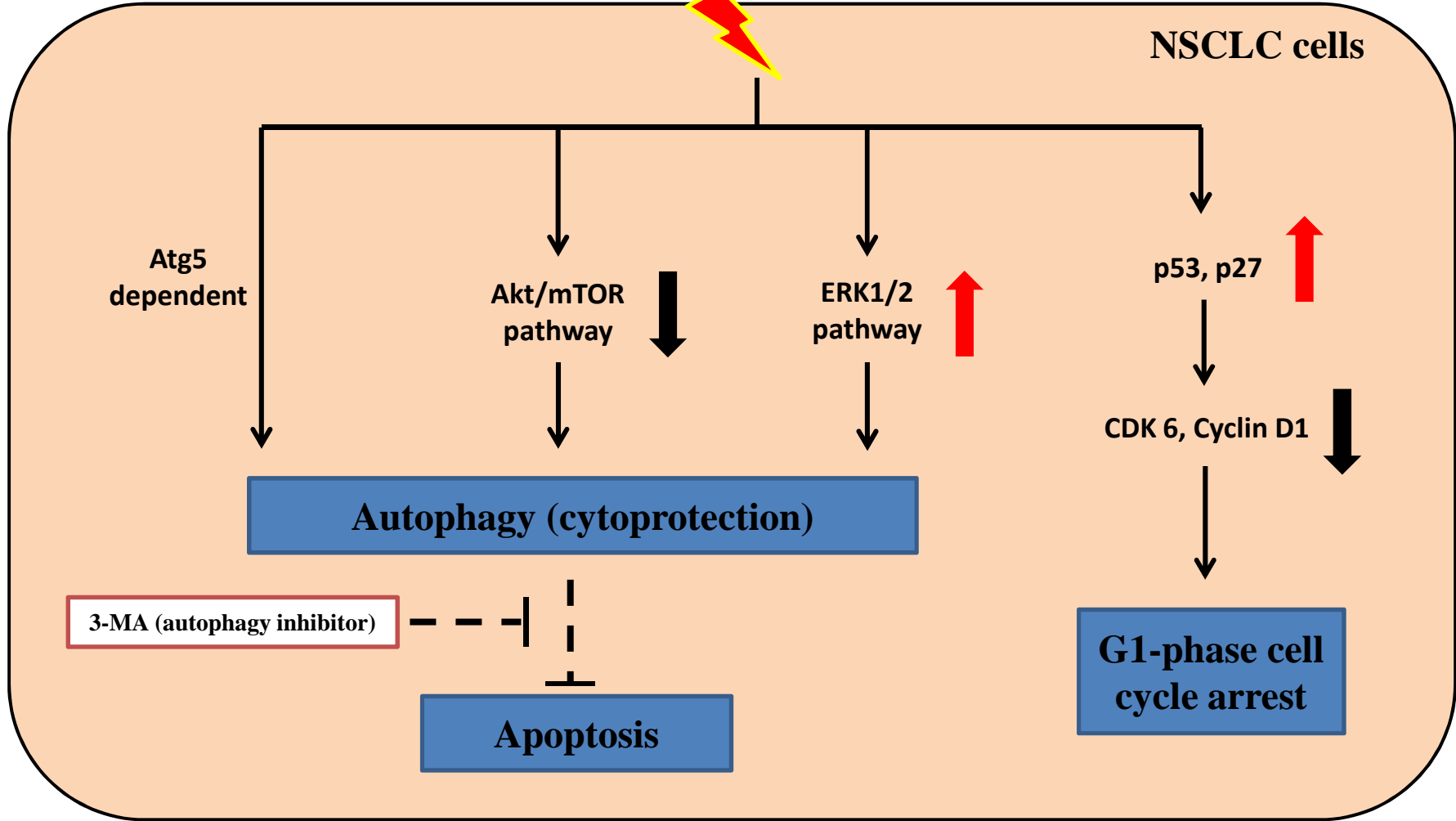
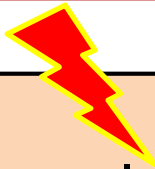


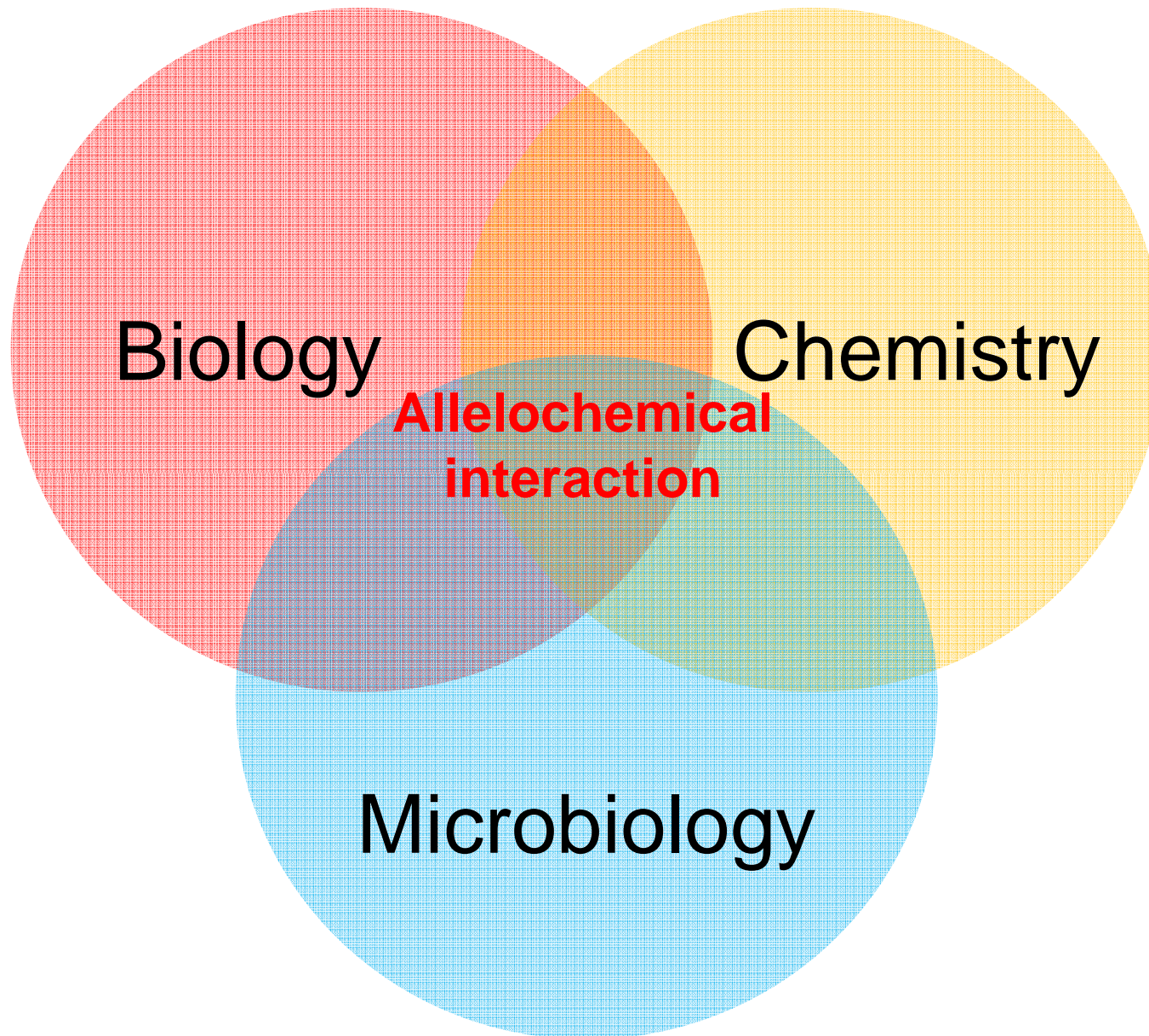
Figure 8. CNT D1 downregulated Akt/mTOR phosphorylation and upregulated ERK1/2 phosphorylation in A549 cells. (A) A549 cells treated with CNT D1 at 125, 150, and 175  $\mu$ M for 72 h. (B) A549 cells were treated with CNT D1 (150  $\mu$ M) for the indicated time. The protein expression of Akt and mTOR phosphorylation was measured by Western blot. (C) A549 cells treated with CNT D1 at 125, 150, and 175  $\mu$ M for 72 h. (D) A549 cells were treated with CNT D1 (150  $\mu$ M) for the indicated time. The protein expression of ERK1/2 and JNK phosphorylation was measured by Western blot. Western blot data presented are representative of those obtained in at least three separate experiments. The values below the figures represent the change in protein expression of the bands normalized to  $\beta$ -actin.



**Cinnamtannin D1**



# Study on Chemical Ecology Needs Multiple Disciplines



# Conclusions

- *Rhododendron formosanum* released varieties of natural products, such as fatty acids, phenolics, flavonoids and terpenoids, etc.
- The aforementioned natural products possess allelopathic, allelochemical, and pharmaceutical properties.
- (-)-catechin and its polymers play a major role in allelopathy and pharmaceutical
- Catechin converted to procatechuic acid through microbial transformation plays the most important role in allelopathic effect upon the growth of understory species



# Conclusions

- **Triterpenoids, namely ursolic acid, oleanolic acid, and betulinic acid, perform anticancer activity on non-small-cell lung carcinoma cells at low concentration of 20  $\mu$ M.**
- **Procyanidins perform anticancer activity on lung cancer cells and antibacterial activity against certain pathogens.**
- **All natural products indicated above are highly potential to be developed into herbicides, fungicide, antibiotics, and pharmaceutical usage.**
- **Natural products from *Rhododendron formosanum* exhibit diverse functions of biodiversity which benefits to human well-being**



# Acknowledgements

- National Science Council, Taiwan
- Research center for biodiversity,  
China Medical University



*Thanks for your attentions*

